Bidirectional contact tracing is required for reliable COVID-19 control

William J. Bradshaw[1], Ethan C. Alley[2,3], Jonathan H. Huggins[4], Alun L. Lloyd[5], and Kevin M. Esvelt[2,*]

[1]Max Planck Institute for Biology of Ageing, Joseph-Stelzmann-Str. 296, 50937 Cologne, Germany
[2]Media Laboratory, Massachusetts Institute of Technology, Cambridge, MA 02139, USA
[3]Alt. Technology Labs, Berkeley, CA 94702, USA
[4]Department of Mathematics & Statistics, Boston University, Boston, MA 02215, USA
[5]Biomathematics Graduate Program and Department of Mathematics, North Carolina State University, Raleigh, NC 27695, USA
* Email: esvelt@mit.edu

Abstract. Contact tracing is critical to limiting the spread of pandemics such as COVID-19, but most protocols only "forward-trace" to notify people who were recently exposed. Using a stochastic branching process model, we find that "bidirectional" tracing to identify infector individuals robustly outperforms forward-only approaches across a wide range of scenarios. The addition of rapid smartphone-based exposure notification offers few benefits over conventional manual tracing alone unless uptake of the digital system is near-universal. However, as long as exposure events can be detected by nearly all smartphones, the combination of manual and digital with bidirectional tracing more than doubles the probability of controlling outbreaks across three epidemiological scenarios. Implementing combined bidirectional tracing may be critical to controlling COVID-19 without more costly interventions.

Introduction

Contact tracing, isolation, and testing are some of the most powerful public health interventions available. The nations that have most effectively controlled the ongoing COVID-19 pandemic are noteworthy for conducting more comprehensive and sophisticated tracing and testing than less successful countries (*1*, *2*). Current "forward-tracing" protocols seek to identify and isolate individuals who were exposed and may have been infected by the index case, thereby preventing continued transmission (Fig. 1a). For example, the European Union protocol calls for the identification of contacts starting two days prior to the development of symptoms (*3*).

However, chains of SARS-CoV-2 transmission may persist despite excellent medical monitoring and forward-tracing programs due to substantial rates of asymptomatic transmission (*4*) (Fig. 1a). Asymptomatic carriers, who reportedly bear equivalent viral loads to patients exhibiting symptoms (*5*), originally estimated at 18% of infected individuals on the Diamond Princess cruise ship (*6*), now include a reported majority of infected sailors on the *Theodore Roosevelt (7)* and 79% of mothers who tested positive in an obstetrics ward in New York (*8*). Population surveys in Italy, Iceland, and China have reported intermediate values around 45% (*9–11*). High rates of asymptomatic carriers might result in undetected transmission chains that could reduce the efficacy of forward-tracing.

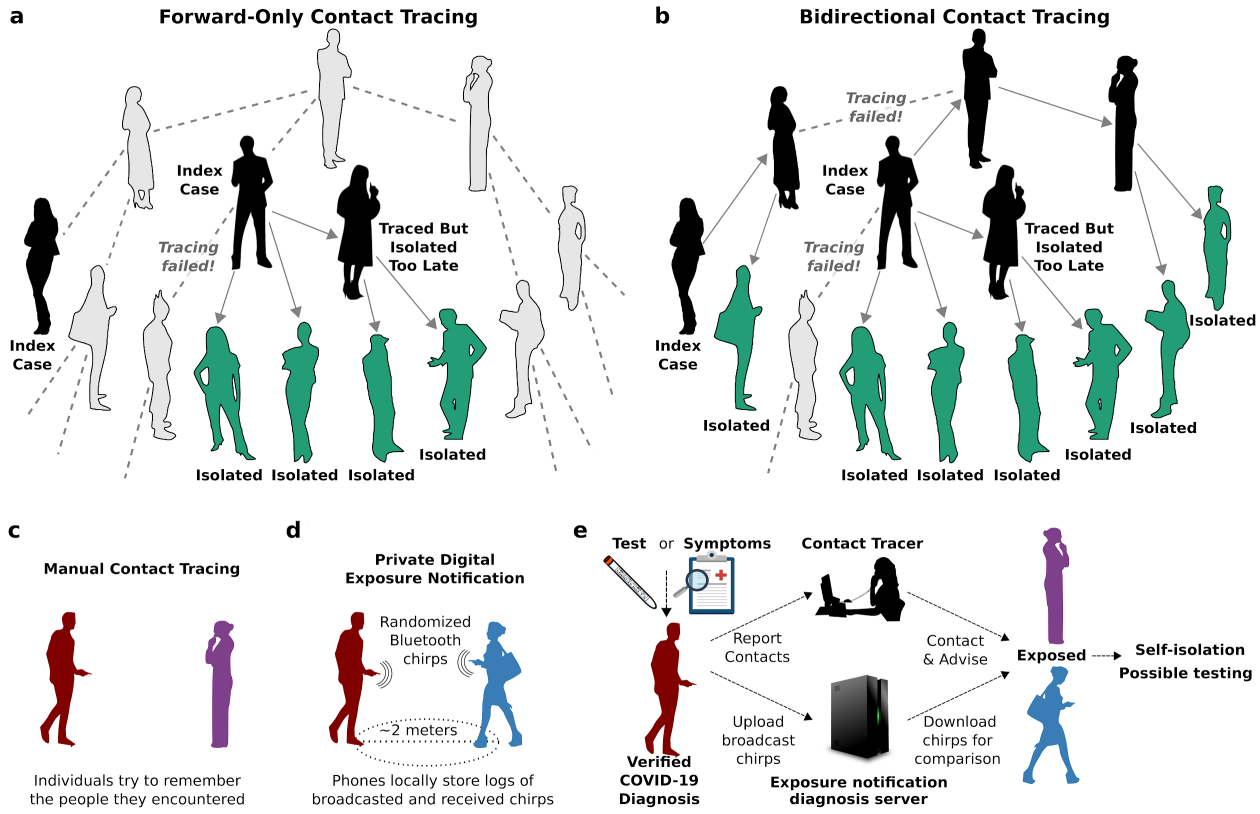

Figure 1. Forward-only and bidirectional contact tracing and digital exposure notification. (a) Notifying people exposed to known cases (black) and isolating them (green) can prevent further transmission, but will miss asymptomatic and undiagnosed cases (gray) and descendants. (b) Bidirectional tracing seeks to also notify and test infectors, enabling the subsequent notification and isolation of asymptomatic and undiagnosed cases and their descendants. (c) Manual contact tracing requires individuals to share a list of the people they have encountered with health authorities, who try to contact each person. (d) Private digital exposure notification apps are being developed by universities and public health authorities with support from Apple and Google, who are incorporating Bluetooth exposure detection capabilities into iOS and Android. Each device will broadcast rotating pseudorandom number "chirps" via Bluetooth and record those emitted by nearby devices, with signal strength indicating proximity (*12*, *13*). (e) In most privacy-preserving designs, individuals diagnosed with COVID-19 would be given a key enabling them to "opt-in" by uploading the chirps they broadcast to a diagnosis server (*14*). All devices will check the server to learn whether any posted numbers match their local exposure log and alert the user of exposure over a threshold set by the health authority. Manual tracers would seek to identify contacts without smartphones.

We hypothesized that when asymptomatic carriers are common, "bidirectional" contact tracing could identify and isolate branches of the viral family tree that would otherwise have gone undiscovered, potentially preventing many additional cases (Fig. 1b). Bidirectional contact tracing uses "reverse-tracing" to identify the parent case who infected an index case, then further forward tracing to iteratively discover other infectees of the parent case.

We further hypothesized that supplementing manual tracing with digital exposure notification would be most effective, as the additional workload for already overburdened tracers would make bidirectional

manual tracing a challenge. Indeed, numerous efforts currently underway aim to supplement manual contact tracing (Fig. 1c) with digital tracing by using smartphones emitting randomized Bluetooth "chirps" to notify people exposed to infected individuals (Fig. 1, d–e). These digital approaches can preserve the privacy of both parties and may also offer considerable advantages in speed (*15*), scale, efficacy (*4*), and confidentiality (*13*, *16–19*).

To determine whether bidirectional tracing could help control transmission, and compare manual and digital approaches, we adapted and extended a stochastic branching process model of SARS-CoV-2 forward-tracing (*20*) and used it to explore the efficacy of different possible combinations of manual contact tracing and digital exposure notification under plausible epidemiological scenarios (Table 1).

Results

Bidirectional tracing improves epidemic control in manual and idealized digital scenarios

In our transmission model, each case generates a number of new cases drawn from a negative binomial distribution, with the time of symptoms onset and exposure determined by incubation and generation distributions based on the published literature. We assume that 90% of symptomatic cases are eventually identified based on symptoms alone, 90% of which comply with isolation requests to prevent further infection. Each outbreak was initialized with 20 index cases, and designated as "controlled" if it reached extinction (zero new cases) before reaching a total of 10,000 cumulative cases (Supplementary Methods). Digital contact tracing is assumed to be instantaneous upon diagnosis, while the time required for manual tracing followed a heavy-tailed distribution with a two-thirds probability of tracing within one day (median 0.5 days) and a minority of cases taking much longer.

We began by investigating a median scenario in which 10% of transmission was assumed to be environmental and therefore untraceable, 48% of transmission occurred pre-symptomatically, and 45% of cases were asymptomatic with reduced contagiousness (Table 1). Testing assumed a sensitivity of 80% (*21*, *22*), and to be capable of detecting both active and past cases (e.g., by serology). For the initial analysis we assumed a fixed basic reproduction number (R_0) of 2.5 but explored other R_0 values below.

In our median scenario, manual contact tracing extending up to 48 hours before symptoms onset per current guidelines (*3*) achieved very low probabilities of control even when all contacts during that window were successfully traced (Fig. 2a). Implementing manual bidirectional tracing with the tracing window extended to 7 days before symptom onset (Fig. S1) substantially improved relative performance, but the best-case probability of control was still 40%. Further widening the tracing window resulted in minimal additional improvement (Fig. S2).

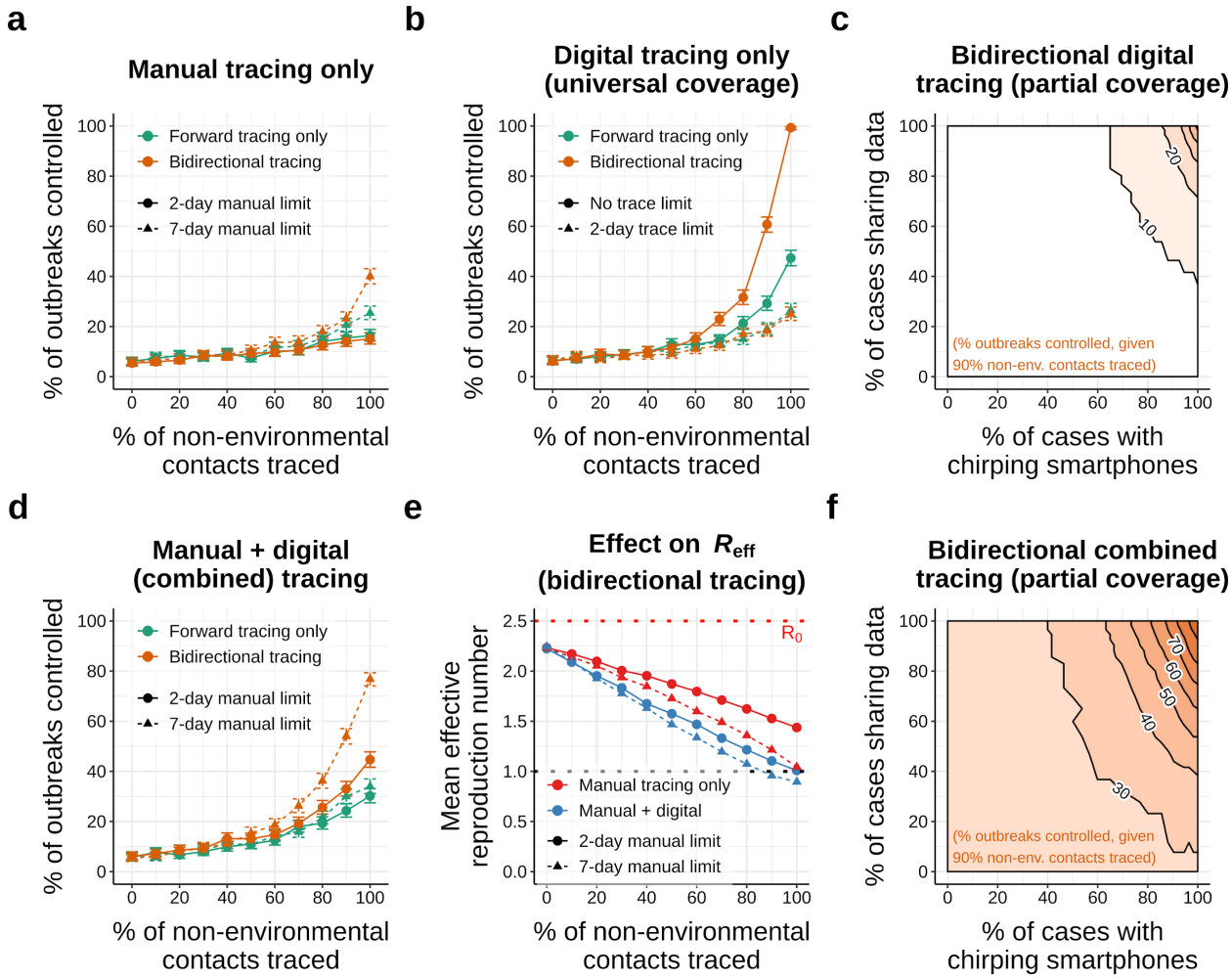

Figure 2. Comparing forward and bidirectional contact tracing at R_0 = 2.5. (a) Percentage of outbreaks controlled by manual contact tracing alone. (b) Percentage of outbreaks controlled using digital tracing alone, assuming universal smartphone coverage and data sharing. (c) Neighbor-averaged contour plot showing percentage of outbreak control for digital-only contact tracing given non-universal chirping smartphone coverage and data-sharing, assuming 90% of non-environmental contacts traced. (d) Percentage of outbreaks controlled by combined manual and digital tracing, assuming 90% data sharing and 80% smartphone usage. (e) Average effective reproduction number achieved by bidirectional manual and combined tracing, as a function of % non-environmental contacts traced. (f) Neighbor-averaged contour plot showing probability of control for combined tracing given non-universal chirping and data-sharing, assuming 90% of non-environmental contacts traced (Methods). Unless otherwise specified, all panels assume median disease parameters (Table 1), including 10% environmental transmission. Error bars in (a,b,d) represent 95% credible intervals across 1000 runs under a uniform prior; points in (e) represent average values over the same.

Compared to manual tracing, digital tracing via smartphone is both faster and scalable to much wider time windows, without being limited by individual memory or the feasible workload of human contact tracers. When all contacts within a 14-day data-retention window were available for analysis (*12*), an ideal digital forward-tracing system with universal upload produced superior outcomes relative to manual forward-tracing (Fig. 2b), in agreement with earlier models (*4*). Crucially, bidirectional tracing exhibited an even more dramatic improvement over the forward-only approach, more than doubling the best-case probability

of successful outbreak control. However, restricting tracing to 48 hours prior to symptom onset, as is widely done for manual contact tracing, significantly impaired performance (Fig. 2b).

Digital tracing is fragile to network fragmentation

Our model's initial predictions for idealized digital contact tracing appear promising. However, these high success rates assumed a comprehensive network of individuals who keep anonymous exposure logs via bluetooth chirping and universally upload their broadcasted chirps when diagnosed with COVID-19. We hypothesized that the effectiveness of digital tracing would rapidly degrade when fewer people participated in the digital system, in line with or worse than the quadratic dependence noted by others (*4*, *13*, *16–18*). To investigate, we modelled epidemic outcomes over a range of smartphone participation and data sharing values (Fig. 2c and Fig. S3). Even small decreases in the proportion of individuals carrying a participating smartphone or (to a lesser extent) choosing to share their broadcasted chirps resulted in fragmentation of the tracing network, reducing probabilities of successful control to levels comparable to, or worse than, manual tracing alone. As a consequence of this fragility to network fragmentation, our results suggest that digital tracing alone cannot substitute for traditional manual tracing, even under very optimistic assumptions about uptake and use (*23*, *24*).

Combining manual and digital tracing improves robustness

Neither manual nor digital contact tracing alone was sufficient to control COVID-19 in our median scenario. Digital tracing is fast and comprehensive but highly fragile to network fragmentation; manual tracing is slower and limited to a narrow time window, but more robust. We therefore hypothesized that the two methods could complement each other, with manual contact tracers focusing their effort on tracing links in the network invisible to the digital system, and that this combined approach might outperform either method in isolation.

We found that combined manual tracing and digital exposure notification resulted in increases in outbreak control probability (Fig. 2d and Fig. S4), roughly doubling control probabilities under bidirectional tracing when the proportion of non-environmental contacts traced was 80% or greater. Even when absolute control probabilities were low, combining automated and manual tracing could substantially reduce the effective reproduction number of the outbreak (Fig. 2e and Fig. S5). Control probability was still somewhat sensitive to the proportion of users with chirping smartphones and proportion of users willing to upload their broadcasted chirps upon becoming infected (Fig. 2f and Fig. S6). However, we found that 50% control could be achieved with combined bidirectional tracing as the only intervention under our median scenario if 80% of cases had chirp-enabled smartphones, and 90% of smartphone users uploaded their broadcasted chirps to notify others.

We additionally modelled the effect of requiring a positive test result before tracing symptomatic cases. This framework is used in various European countries among others (*3*) and contradicts our assumption

that symptomatic cases are traced immediately upon diagnosis, with only asymptomatic or presymptomatic cases requiring a test (Supplementary Methods). Reproducing Figure 2e–f under this framework, we observed a moderate decrease in control probability even given a fast test turnaround time averaging one day, with best-case control probabilities falling from 79% to 57% (Fig. S7). This finding is consistent with previous modelling studies reporting impaired performance under these conditions (*25*).

High-uptake combined bidirectional tracing robustly doubles the probability of outbreak control

Epidemiological parameters for COVID-19 remain highly uncertain. Among these, R_0 has both wide ranges in published estimates (*4*, *10*, *26–29*) and is expected to have large effects on outbreak outcome. To evaluate the robustness of our findings, we repeated our analysis of different contact-tracing approaches under R_0 values ranging from 1.0 to 4.0 (Fig. 3, a–b). We assumed that 90% non-environmental contacts were traced, a 7-day manual trace window, immediate tracing of symptomatic cases, and (in the digital and combined cases) high uptake of the digital system. A wider range of assumptions are explored in Figures S8–S15, while Figures S16-20 explore the effect of varying different model parameters in isolation.

Small reductions in R_0 resulted in large increases in probability of successful control across all forms of tracing, with a change in R_0 of 0.5 frequently changing the probability by a factor of 2 or more (Fig. 3a). Combined bidirectional tracing robustly outperformed all other tracing strategies, with the greatest degree of outperformance observed when R_0 was between roughly 1.75 and 3.5. Below $R_0 = 1.75$, manual and combined tracing both achieved nearly 100% control, while above $R_0 = 3.5$, no form of tracing achieved control probabilities over 10%. Even in these low-control scenarios, however, combined bidirectional tracing consistently resulted in lower effective reproduction numbers than other forms of tracing (Fig. 3b), with a reduction in R_{eff} of roughly 20% relative to manual tracing alone (Fig. S21).

In all cases, restricting the intervention to forward tracing alone, constraining manual tracing to a 2- rather than 7-day window, or requiring a positive test result before tracing symptomatic cases substantially impaired performance within the critical window of R_0 values (Fig. 3, a–b, and Figs. S8–S14), underscoring the importance of rapid, effective bidirectional tracing. Lowering uptake of the digital system from 80% to 53% of cases – in line with existing survey data (*23–25*) and plans for opt-in chirping participation (*12*) – largely abrogated the advantage of combined over manual approaches (Fig. S15).

Our median estimates of the epidemiological parameters defining COVID-19 suggest a challenging disease to control, with high rates of asymptomatic and pre-symptomatic transmission and low but significant rates of environmental transmission. The exact values of these parameters are highly uncertain, but substantially affect the difficulty. To explore a realistic range of scenarios, we aggregated our collective best estimates to define optimistic and pessimistic values for these parameters (Table 1) and repeated our simulations for a range of R_0 values (Fig. 3, c–f).

Relatively small changes in each of the critical parameters led to substantial differences in the probability of control (Fig. 3). In the optimistic scenario, our model agrees with earlier reports that contact tracing might be sufficient to reliably (i.e., with probability at least 0.9) control the pandemic without other interventions (*4*), but only if $R_0 \leq 2.5$, highly efficient combined bidirectional tracing is used, and nearly 80% of individuals carry chirping smartphones (Fig. 3c). In the median scenario, R_0 must be at most 2.0 to reliably control the outbreak, while in the pessimistic scenario, R_0 must be at most 1.75, both of which are below commonly accepted values in the absence of other interventions.

Comparing the effects of tracing on the effective reproduction number of the epidemic, we observed that combined bidirectional tracing reduced R_{eff} by roughly 25% in the optimistic, 20% in the median and 15% in the pessimistic scenarios relative to manual tracing alone (Fig. 3, b,d,f, and Figs. S21 and S23), and by roughly 65% in the optimistic,

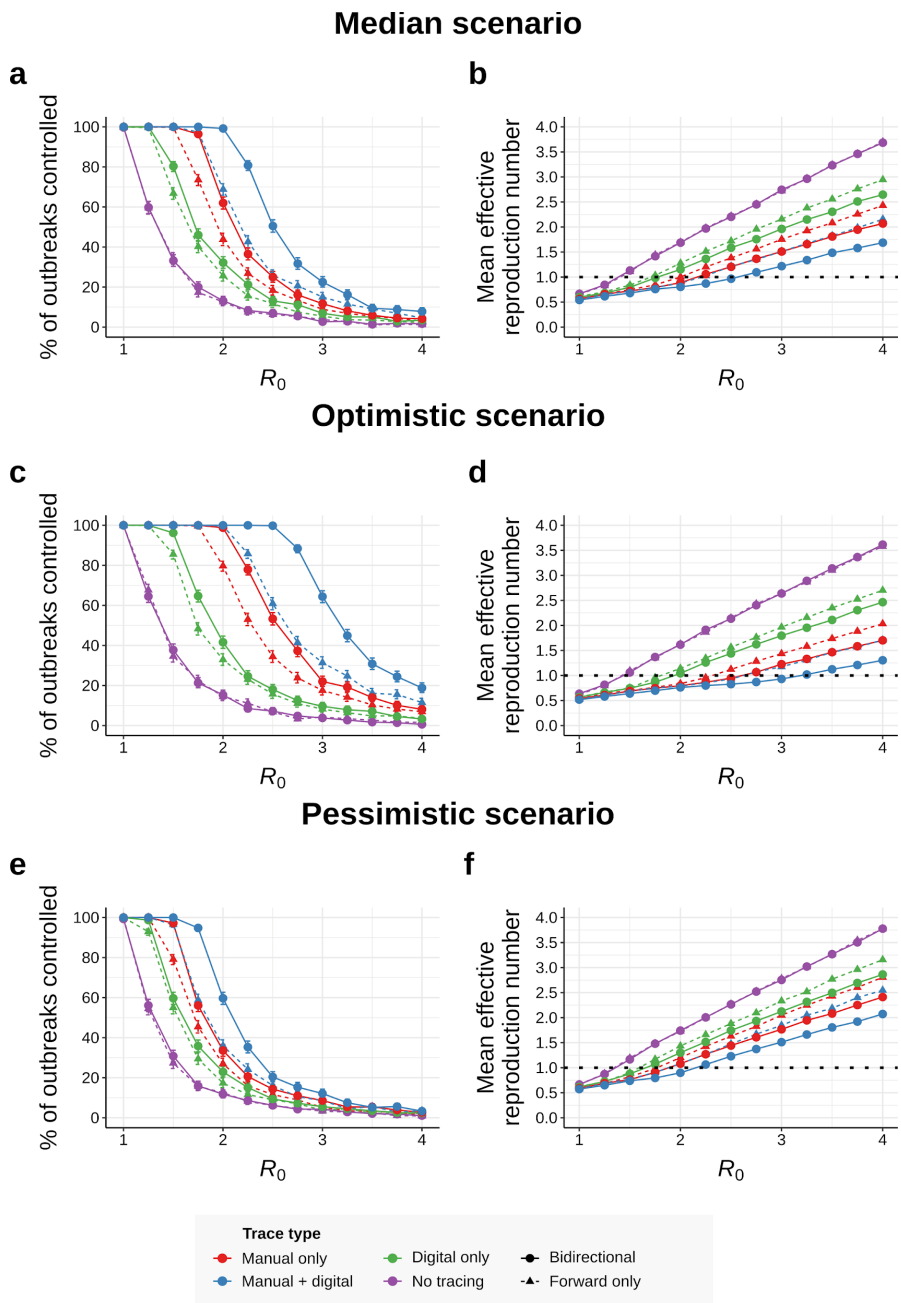

Figure 3. Effect of R_0 and disease parameters on performance. (a,c,e) Percentage of outbreaks controlled and (b,d,f) average effective reproduction number under various forms of contact tracing (manual, digital, both or neither; forward-only or bidirectional) as a function of the basic reproduction number R_0, assuming median, optimistic or pessimistic disease parameters (Table 1), 90% non-environmental contacts traced, and a 7-day manual trace window. Error bars in (a,c,e) represent 95% credible intervals across 1000 runs under a uniform beta prior; points in (b,d,f) represent average values over the same. Isolating symptomatics can dampen the outbreak at low R_0, even in the absence of tracing.

55% in the median and 45% in the pessimistic scenarios relative to no tracing at all (Figs. S22 and S24). Since any R_{eff} value below 1 results in the eventual extinction of the outbreak, the combination of effective manual and digital tracing might be capable of single-handedly controlling the COVID-19 pandemic in the optimistic scenario; and, if combined with other measures to reduce R_{eff} such as masks, hygiene, or physical distancing (*30*), could likely do the same even under our pessimistic assumptions.

To summarize the predicted effects of different possible contact tracing implementations, we compared the probability of controlling COVID-19 with tracing alone under all three scenarios (median, optimistic, and pessimistic), assuming an R_0 value of 2.5, 90% of non-environmental contacts traced, and a 7-day manual tracing window (Fig. 4). In the pessimistic scenario, no tracing strategy was sufficient in isolation, although all reduced R_{eff} by varying amounts (Fig. S25). Both manual tracing and digital exposure notification alone failed to reliably control the epidemic in the median and pessimistic scenarios. Low uptake of the digital system largely precluded its utility, while combined bidirectional tracing with high digital uptake offered even odds of control in the median scenario and near certainty of control in the optimistic scenario. Relative to current manual tracing approaches, combined bidirectional tracing with high uptake more than doubled the probability of controlling the spread SARS-CoV-2 across all scenarios.

Discussion

Given the tremendous suffering inflicted by the COVID-19 pandemic, the potentially critical role of expanding contact tracing systems, and the ongoing development of exposure notification apps by universities and public health authorities of diverse nations that could supplement and expand the reach of manual tracing, there is an urgent need to address questions concerning the optimal implementation of these systems.

Our stochastic model extends existing approaches, incorporating distinctions between manual and digital strategies (Fig. 2) and updated estimates of key epidemiological parameters. We stress-tested our conclusions with a wide range of plausible parameter combinations and possible values of R_0 (Figs. 3–4). Notably, our "optimistic" scenario is more pessimistic than many earlier studies of contact tracing because we assume higher values for both the rate and relative infectiousness of asymptomatic carriers based on numerous recent studies (*5*, *10*, *27*, *31–33*).

Our model predicts that current plans to supplement forward manual contact tracing with an opt-in digital forward-tracing system will fail. Manual systems outperform digital equivalents unless almost every resident has a participating smartphone (Fig. 2, a–c, Fig. 4, and Figs. S15 and S25–27), and even combined approaches offer only marginal improvements at levels of participation predicted by surveys (*23–25*) (Fig. 4, low uptake). Even if exposure events are detectable by nearly all smartphones, adding digital to manual forward-tracing achieves only minor benefits.

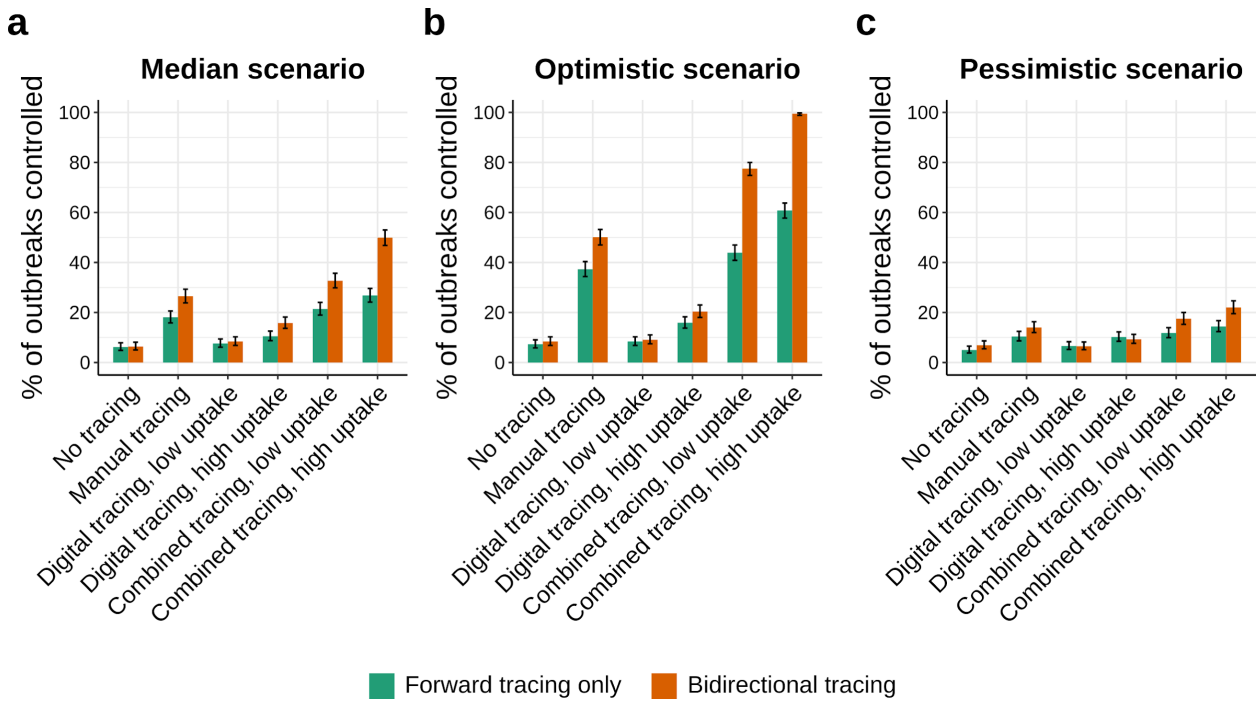

Figure 4. Bidirectional digital+manual tracing doubles the probability of controlling COVID-19 over forward-only manual tracing across scenarios. Percentage of outbreaks controlled under median (a), optimistic (b), and pessimistic (c) scenarios (Table 1), assuming an R_0 of 2.5, 90% of non-environmental contacts traced, 7-day manual tracing windows, and immediate (pre-test) tracing of symptomatic cases. Without tracing, forward and bidirectional are equivalent.

We find that bidirectional tracing is key to effectively controlling SARS-CoV-2. Indeed, for a combined manual+digital tracing system to reach the levels of control cited by earlier, more optimistic studies (*4*, *25*), we find that bidirectional tracing is *required*. Bidirectional tracing outperforms forward-tracing regardless of how the tracing is done, and bidirectional manual+digital tracing with high uptake is predicted to be more than twice as effective at controlling outbreaks as manual forward-tracing alone across all scenarios (Figs. 3–4).

Combining bidirectional tracing with a hybrid manual+digital tracing strategy was sufficient to reliably control the pandemic without other interventions under optimistic assumptions (Fig. 4). However, even this strategy offered only 50–50 odds in our median scenario with an R_0 of 2.5 (Figs. 3–4). If low-cost precautions can reduce R_{eff} below 1.75 (*30*), our model predicts that a combined, high-uptake bidirectional tracing strategy would bring transmission under control with high probability even under our pessimistic scenario (Fig. 3, e–f). Hence, society could avoid much more costly control measures. To achieve these benefits, manual contact tracing should be made explicitly bidirectional, and the manual tracing window expanded as far as resources allow – ideally to 7 days before symptom onset (Fig. 2d & Fig. S5). This larger window could be made feasible by leveraging the lightened workload afforded by the digital system handling most contacts.

While our model is less idealized than its predecessors, it nevertheless has limitations. In particular, it makes no distinction between mildly and severely symptomatic cases – either in infectiousness or in test sensitivity over time – and does not consider differences in age, location, behavior, or other causes of variation between cases. Only the sensitivity of testing is considered; in reality, the balance between test sensitivity and specificity is a crucial trade-off, and high rates of false positives will severely impede response effectiveness and the credibility of the tracing system.

Whether our conclusions are borne out in practice depends on the feasibility of privacy-respecting exposure notification systems that implement efficient bidirectional tracing algorithms capable of acceptable sensitivity and specificity (*12*) and whether voluntary data-sharing can reach sufficient levels. A successful control program also depends on the availability of adequate COVID-19 testing (*21*, *34*), high compliance with isolation requests (*4*, *20*, *35*, *36*), and scaling of manual contact tracing (*37*). Those caveats aside, our results indicate that if nearly all smartphones can detect exposure events, bidirectional digital+manual contact tracing can play an essential and potentially decisive role in controlling COVID-19 and preventing future pandemics.

Acknowledgments

We thank Aaron Bucher of the COVID-19 HPC Consortium and Amazon Web Services for granting us extra cloud compute credits.

Funding: This work was supported by gifts from the Reid Hoffman Foundation and the Open Philanthropy Project (to K.M.E.) and cluster time granted by the COVID-19 HPC-1 consortium (MCB20071 to K.M.E.). E.C.A. was supported by a fellowship from the Open Philanthropy Project. A.L.L. is supported by the Drexel Endowment (NC State University).

Author Contributions: K.M.E. conceived the study. J.H.H. and A.L.L. identified a suitable model framework. W.J.B. designed and programmed the adapted model, advised by the other authors. All authors independently estimated key model parameters based on the literature. W.J.B. ran all simulations and generated figures with assistance from E.C.A. All authors jointly wrote and edited the manuscript.

Data and Code Availability: Code for configuring and running the model is publicly available at https://github.com/willbradshaw/covid-bidirectional-tracing.

References

1. J. Cohen, K. Kupferschmidt, Countries test tactics in "war" against COVID-19. *Science*. **367**, 1287–1288 (2020).

2. Y. Huang, M. Sun, Y. Sui, How Digital Contact Tracing Slowed Covid-19 in East Asia. *Harvard Business Review* (2020), (available at https://hbr.org/2020/04/how-digital-contact-tracing-slowed-covid-19-in-east-asia).

3. Contact tracing: Public health management of persons, including healthcare workers, having had contact with COVID-19 cases in the European Union - second update. *European Centre for Disease Prevention and Control* (2020), (available at https://www.ecdc.europa.eu/en/covid-19-contact-tracing-public-health-management).

4. L. Ferretti, C. Wymant, M. Kendall, L. Zhao, A. Nurtay, L. Abeler-Dörner, M. Parker, D. Bonsall, C. Fraser, Quantifying SARS-CoV-2 transmission suggests epidemic control with digital contact tracing. *Science* (2020), doi:10.1126/science.abb6936.

5. L. Zou, F. Ruan, M. Huang, L. Liang, H. Huang, Z. Hong, J. Yu, M. Kang, Y. Song, J. Xia, Q. Guo, T. Song, J. He, H.-L. Yen, M. Peiris, J. Wu, SARS-CoV-2 Viral Load in Upper Respiratory Specimens of Infected Patients. *N. Engl. J. Med.* **382**, 1177–1179 (2020).

6. K. Mizumoto, K. Kagaya, A. Zarebski, G. Chowell, Estimating the asymptomatic proportion of coronavirus disease 2019 (COVID-19) cases on board the Diamond Princess cruise ship, Yokohama, Japan, 2020. *Euro Surveill.* **25** (2020), doi:10.2807/1560-7917.ES.2020.25.10.2000180.

7. D. S. Correll, SECDEF: Majority of Roosevelt sailors with COVID-19 are asymptomatic. *Navy Times* (2020), (available at https://www.navytimes.com/news/coronavirus/2020/04/16/secdef-majority-of-roosevelt-sailors-with-covid-19-are-asymptomatic-flattop-still-wartime-ready/).

8. D. Sutton, K. Fuchs, M. D'Alton, D. Goffman, Universal Screening for SARS-CoV-2 in Women Admitted for Delivery. *N. Engl. J. Med.* (2020), doi:10.1056/NEJMc2009316.

9. D. F. Gudbjartsson, A. Helgason, H. Jonsson, O. T. Magnusson, P. Melsted, G. L. Norddahl, J. Saemundsdottir, A. Sigurdsson, P. Sulem, A. B. Agustsdottir, B. Eiriksdottir, R. Fridriksdottir, E. E. Gardarsdottir, G. Georgsson, O. S. Gretarsdottir, K. R. Gudmundsson, T. R. Gunnarsdottir, A. Gylfason, H. Holm, B. O. Jensson, A. Jonasdottir, F. Jonsson, K. S. Josefsdottir, T. Kristjansson, D. N. Magnusdottir, L. le Roux, G. Sigmundsdottir, G. Sveinbjornsson, K. E. Sveinsdottir, M. Sveinsdottir, E. A. Thorarensen, B. Thorbjornsson, A. Löve, G. Masson, I. Jonsdottir, A. D. Möller, T. Gudnason, K. G. Kristinsson, U. Thorsteinsdottir, K. Stefansson, Spread of SARS-CoV-2 in the Icelandic Population. *N. Engl. J. Med.* (2020), doi:10.1056/NEJMoa2006100.

10. E. Lavezzo, E. Franchin, C. Ciavarella, G. Cuomo-Dannenburg, L. Barzon, C. Del Vecchio, L. Rossi, R. Manganelli, A. Loregian, N. Navarin, D. Abate, M. Sciro, S. Merigliano, E. Decanale, M. C. Vanuzzo, F. Saluzzo, F. Onelia, M. Pacenti, S. Parisi, G. Carretta, D. Donato, L. Flor, S. Cocchio, G. Masi, A. Sperduti, L. Cattarino, R. Salvador, K. A. M. Gaythorpe, Imperial College London COVID-19 Response Team, A. R. Brazzale, S. Toppo, M. Trevisan, V. Baldo, C. A. Donnelly, N. M. Ferguson, I. Dorigatti, A. Crisanti, Suppression of COVID-19 outbreak in the municipality of Vo, Italy. *medRxiv* (2020), , doi:10.1101/2020.04.17.20053157.

11. S. Ma, J. Zhang, M. Zeng, Q. Yun, W. Guo, Y. Zheng, S. Zhao, M. H. Wang, Z. Yang, Epidemiological parameters of coronavirus disease 2019: a pooled analysis of publicly reported individual data of 1155 cases from seven countries. *medRxiv* (2020), doi:10.1101/2020.03.21.20040329.

12. Keyword Team, Apple and Google partner on COVID-19 contact tracing technology. *Google* (2020), (available at https://blog.google/inside-google/company-announcements/apple-and-google-partner-covid-19-contact-tracing-technology/).

13. Rivest R, Weitzner D, Kalai Y, Raskar R, Gruber J, Esvelt KM, Vepakomma P, Zeldovich N, Abelson H, A simple proximity-based approach to contact tracing (2020) (available at https://epic.org/privacy/covid/Rivest-Contact-Tracing.pdf).

14. "Exposure Notification FAQ v1.0" (Google, 2020), (available at https://www.blog.google/documents/63/Exposure_Notification_-_FAQ_v1.0.pdf).

15. J. Müller, B. Koopmann, The effect of delay on contact tracing. *Math. Biosci.* **282**, 204–214 (2016).

16. R. Canetti, A. Trachtenberg, M. Varia, Anonymous Collocation Discovery: Harnessing Privacy to Tame the Coronavirus. *arXiv e-prints*, arXiv:2003.13670 (2020).

17. H. Reed, TCN Coalition · A Global Coalition for Privacy-First Digital Contact Tracing Protocols to Fight COVID-19, (available at https://tcn-coalition.org/).

18. DP^3T Consortium, Decentralized Privacy-Preserving Contact Tracing. *Github*, (available at https://github.com/DP-3T).

19. CovidSafe, (available at https://covidsafe.cs.washington.edu/).

20. J. Hellewell, S. Abbott, A. Gimma, N. I. Bosse, C. I. Jarvis, T. W. Russell, J. D. Munday, A. J. Kucharski, W. J. Edmunds, Centre for the Mathematical Modelling of Infectious Diseases COVID-19 Working Group, S. Funk, R. M. Eggo, Feasibility of controlling COVID-19 outbreaks by isolation of cases and contacts. *Lancet Glob Health*. **8**, e488–e496 (2020).

21. J. Zhao, Q. Yuan, H. Wang, W. Liu, X. Liao, Y. Su, X. Wang, J. Yuan, T. Li, J. Li, S. Qian, C. Hong, F. Wang, Y. Liu, Z. Wang, Q. He, Z. Li, B. He, T. Zhang, Y. Fu, S. Ge, L. Liu, J. Zhang, N. Xia, Z. Zhang, Antibody responses to SARS-CoV-2 in patients of novel coronavirus disease 2019. *Clin. Infect. Dis.* (2020), doi:10.1093/cid/ciaa344.

22. J. D. Whitman, J. Hiatt, C. T. Mowery, B. R. Shy, R. Yu, T. N. Yamamoto, U. Rathore, G. M. Goldgof, C. Whitty, J. M. Woo, A. E. Gallman, T. E. Miller, A. G. Levine, D. N. Nguyen, S. P. Bapat, J. Balcerek, S. Bylsma, A. M. Lyons, S. Li, A. W.-Y. Wong, E. M. Gillis-Buck, Z. B. Steinhart, Y. Lee, R. Apathy, M. J. Lipke, J. A. Smith, T. Zheng, I. C. Boothby, E. Isaza, J. Chan, D. D. Acenas II, J. Lee, T. A. Macrae, T. S. Kyaw, D. Wu, D. L. Ng, W. Gu, V. A. York, H. A. Eskandarian, P. C. Callaway, L. Warrier, M. E. Moreno, J. Levan, L. Torres, L. Farrington, R. Loudermilk, K. Koshal, K. C. Zorn, W. F. Garcia-Beltran, D. Yang, M. G. Astudillo, B. E. Bernstein, J. A. Gelfand, E. T. Ryan, R. C. Charles, A. J. Iafrate, J. K. Lennerz, S. Miller, C. Y. Chiu, S. L. Stramer, M. R. Wilson, A. Manglik, C. J. Ye, N. J. Krogan, M. S. Anderson, J. G. Cyster, J. D. Ernst, A. H. B. Wu, K. L. Lynch, C. Bern, P. D. Hsu, A. Marson, Test performance evaluation of SARS-CoV-2 serological assays. *medRxiv* (2020), doi:10.1101/2020.04.25.20074856.

23. KFF Health Tracking Poll – Late April 2020: Coronavirus, Social Distancing, and Contact Tracing. *The Henry J. Kaiser Family Foundation* (2020), (available at https://www.kff.org/global-health-policy/issue-brief/kff-health-tracking-poll-late-april-2020/).

24. E. Hargittai, E. Redmiles, Will Americans Be Willing to Install COVID-19 Tracking Apps? *Scientific American Blog Network*, (available at https://blogs.scientificamerican.com/observations/will-americans-be-willing-to-install-covid-19-tracking-apps/).

25. Hinch R, Probert W, Nurtay A, Kendall M, Wymant C, Hall M, Lythgoe K, Bulas Cruz A, Zhao L,

Stewart A, Ferretti L, Parker M, Meroueh A, Mathias B, Stevenson S, Montero D, Warren J, Mather NK, Finkelstein A, Abeler-Dorner L, Bonsall D, Fraser C, Effective configurations of a digtal contact tracing app: A report to NHSX (2020), (available at https://github.com/BDI-pathogens/covid-19_instant_tracing).

26. A. J. Kucharski, P. Klepac, A. Conlan, S. M. Kissler, M. Tang, H. Fry, J. Gog, J. Edmunds, CMMID COVID-19 Working Group, Effectiveness of isolation, testing, contact tracing and physical distancing on reducing transmission of SARS-CoV-2 in different settings. *medRxiv* (2020), doi:10.1101/2020.04.23.20077024.

27. R. Li, S. Pei, B. Chen, Y. Song, T. Zhang, W. Yang, J. Shaman, Substantial undocumented infection facilitates the rapid dissemination of novel coronavirus (SARS-CoV-2). *Science*. **368**, 489–493 (2020).

28. Q. Li, X. Guan, P. Wu, X. Wang, L. Zhou, Y. Tong, R. Ren, K. S. M. Leung, E. H. Y. Lau, J. Y. Wong, X. Xing, N. Xiang, Y. Wu, C. Li, Q. Chen, D. Li, T. Liu, J. Zhao, M. Liu, W. Tu, C. Chen, L. Jin, R. Yang, Q. Wang, S. Zhou, R. Wang, H. Liu, Y. Luo, Y. Liu, G. Shao, H. Li, Z. Tao, Y. Yang, Z. Deng, B. Liu, Z. Ma, Y. Zhang, G. Shi, T. T. Y. Lam, J. T. Wu, G. F. Gao, B. J. Cowling, B. Yang, G. M. Leung, Z. Feng, Early Transmission Dynamics in Wuhan, China, of Novel Coronavirus-Infected Pneumonia. *N. Engl. J. Med.* **382**, 1199–1207 (2020).

29. F. Riccardo, M. Ajelli, X. Andrianou, A. Bella, M. Del Manso, M. Fabiani, S. Bellino, S. Boros, A. Mateo Urdiales, V. Marziano, M. C. Rota, A. Filia, F. (paolo) D'Ancona, A. Siddu, O. Punzo, F. Trentini, G. Guzzetta, P. Poletti, P. Stefanelli, M. R. Castrucci, A. Ciervo, C. Di Benedetto, M. Tallon, A. Piccioli, S. Brusaferro, G. Rezza, S. Merler, P. Pezzotti, COVID-19 working group, Epidemiological characteristics of COVID-19 cases in Italy and estimates of the reproductive numbers one month into the epidemic. *medRxiv* (2020), doi:10.1101/2020.04.08.20056861.

30. J. Zhang, M. Litvinova, Y. Liang, Y. Wang, W. Wang, S. Zhao, Q. Wu, S. Merler, C. Viboud, A. Vespignani, M. Ajelli, H. Yu, Changes in contact patterns shape the dynamics of the COVID-19 outbreak in China. *Science* (2020), doi:10.1126/science.abb8001.

31. Z. Hu, C. Song, C. Xu, G. Jin, Y. Chen, X. Xu, H. Ma, W. Chen, Y. Lin, Y. Zheng, J. Wang, Z. Hu, Y. Yi, H. Shen, Clinical characteristics of 24 asymptomatic infections with COVID-19 screened among close contacts in Nanjing, China. *Sci. China Life Sci.* **63**, 706–711 (2020).

32. B. Cao, Y. Wang, D. Wen, W. Liu, J. Wang, G. Fan, L. Ruan, B. Song, Y. Cai, M. Wei, X. Li, J. Xia, N. Chen, J. Xiang, T. Yu, T. Bai, X. Xie, L. Zhang, C. Li, Y. Yuan, H. Chen, H. Li, H. Huang, S. Tu, F. Gong, Y. Liu, Y. Wei, C. Dong, F. Zhou, X. Gu, J. Xu, Z. Liu, Y. Zhang, H. Li, L. Shang, K. Wang, K. Li, X. Zhou, X. Dong, Z. Qu, S. Lu, X. Hu, S. Ruan, S. Luo, J. Wu, L. Peng, F. Cheng, L. Pan, J. Zou, C. Jia, J. Wang, X. Liu, S. Wang, X. Wu, Q. Ge, J. He, H. Zhan, F. Qiu, L. Guo, C. Huang, T. Jaki, F. G. Hayden, P. W. Horby, D. Zhang, C. Wang, A Trial of Lopinavir-Ritonavir in Adults Hospitalized with Severe Covid-19. *N. Engl. J. Med.* (2020), doi:10.1056/NEJMoa2001282.

33. N. V. V. Chau, V. T. Lam, N. T. Dung, L. M. Yen, N. N. Q. Minh, L. M. Hung, N. M. Ngoc, N. T. Dung, D. N. H. Man, L. A. Nguyet, L. T. H. Nhat, L. N. T. Nhu, N. T. H. Ny, N. T. T. Hong, E. Kestelyn, N. T. P. Dung, N. T. Phong, T. C. Xuan, T. T. Hien, T. N. H. Tu, R. B. Geskus, T. T. Thanh, N. T. Truong, N. T. Binh, T. C. Thuong, G. Thwaites, L. Van Tan, The natural history and transmission potential of asymptomatic SARS-CoV-2 infection. *medRxiv* (2020), doi:10.1101/2020.04.27.20082347.

34. COVID-19 Testing Project, (available at https://covidtestingproject.org/index.html).

35. M. Kretzschmar, G. Rozhnova, M. van Boven, Effectiveness of Isolation and Contact Tracing for Containment and Slowing Down a COVID-19 Epidemic: A Modelling Study (2020).

36. C. M. Peak, R. Kahn, Y. H. Grad, L. M. Childs, R. Li, M. Lipsitch, C. O. Buckee, Comparative Impact of Individual Quarantine vs. Active Monitoring of Contacts for the Mitigation of COVID-19: a modelling study. *medRxiv* (2020), doi:10.1101/2020.03.05.20031088.

37. Reuters, New York to Hire Thousands of Contact Tracers, Reduce Subway Service to Clean Trains. *The New York Times* (2020), (available at https://www.nytimes.com/reuters/2020/04/30/us/30reuters-health-coronavirus-usa-new-york-cuomo.html).

38. Jing Cai, Wenjie Sun, Jianping Huang, Michelle Gamber, Jing Wu, Guiqing He, Indirect Virus Transmission in Cluster of COVID-19 Cases, Wenzhou, China, 2020. *Emerging Infectious Disease journal*. **26** (2020), doi:10.3201/eid2606.200412.

39. H.-Y. Cheng, S.-W. Jian, D.-P. Liu, T.-C. Ng, W.-T. Huang, H.-H. Lin, Taiwan COVID-19 Outbreak Investigation Team, Contact Tracing Assessment of COVID-19 Transmission Dynamics in Taiwan and Risk at Different Exposure Periods Before and After Symptom Onset. *JAMA Intern. Med.* (2020), doi:10.1001/jamainternmed.2020.2020.

40. X. He, E. H. Y. Lau, P. Wu, X. Deng, J. Wang, X. Hao, Y. C. Lau, J. Y. Wong, Y. Guan, X. Tan, X. Mo, Y. Chen, B. Liao, W. Chen, F. Hu, Q. Zhang, M. Zhong, Y. Wu, L. Zhao, F. Zhang, B. J. Cowling, F. Li, G. M. Leung, Temporal dynamics in viral shedding and transmissibility of COVID-19. *Nat. Med.* (2020), doi:10.1038/s41591-020-0869-5.

41. Q.-L. Jing, M.-J. Liu, J. Yuan, Z.-B. Zhang, A.-R. Zhang, N. E. Dean, L. Luo, M.-M. Ma, I. Longini, E. Kenah, Y. Lu, Y. Ma, N. Jalali, L.-Q. Fang, Z.-C. Yang, Y. Yang, Household Secondary Attack Rate of COVID-19 and Associated Determinants. *medRxiv* (2020), doi:10.1101/2020.04.11.20056010.

42. Zhanwei Du, Xiaoke Xu, Ye Wu, Lin Wang, Benjamin J. Cowling, Lauren Ancel Meyers, Serial Interval of COVID-19 among Publicly Reported Confirmed Cases. *Emerging Infectious Disease journal*. **26** (2020), doi:10.3201/eid2606.200357.

43. W. E. Wei, Z. Li, C. J. Chiew, S. E. Yong, M. P. Toh, V. J. Lee, Presymptomatic Transmission of SARS-CoV-2 - Singapore, January 23-March 16, 2020. *MMWR Morb. Mortal. Wkly. Rep.* **69**, 411–415 (2020).

44. T. Ganyani, C. Kremer, D. Chen, A. Torneri, C. Faes, J. Wallinga, N. Hens, Estimating the generation interval for coronavirus disease (COVID-19) based on symptom onset data, March 2020. *Eurosurveillance*. **25**, 2000257 (2020).

45. Demographics of Mobile Device Ownership and Adoption in the United States. *Pew Research Center: Internet, Science & Tech*, (available at https://www.pewresearch.org/internet/fact-sheet/mobile/).

46. A. Harmon, Inside the Race to Contain America's First Coronavirus Case. *The New York Times* (2020), (available at https://www.nytimes.com/2020/02/05/us/corona-virus-washington-state.html).

47. A. Endo, Centre for the Mathematical Modelling of Infectious Diseases COVID-19 Working Group, S. Abbott, A. J. Kucharski, S. Funk, Estimating the overdispersion in COVID-19 transmission using outbreak sizes outside China. *Wellcome Open Res*. **5**, 67 (2020).

48. S. A. Lauer, K. H. Grantz, Q. Bi, F. K. Jones, Q. Zheng, H. Meredith, A. S. Azman, N. G. Reich, J. Lessler, The incubation period of 2019-nCoV from publicly reported confirmed cases: estimation and application. *medRxiv* (2020), doi:10.1101/2020.02.02.20020016.

49. L. McCann, W. Allan, P. Read, A. McNulty, Contact tracing using provider referral: how difficult is it? *Sex. Health*. **10**, 472–473 (2013).

Table 1: Key parameters of the branching-process model.

Parameter	Value			Sources and Notes
	Median	Optimistic	Pessimistic	
% asymptomatic carriers	45%	40%	55%	(*9–11*)
Relative infectiousness of asymptomatic carriers	50%	45%	60%	Informed by viral load measurements and tracing results described in (*5*, *10*, *27*, *31–33*)
% environmental transmission	10%	5%	15%	(*4*, *38*)
Proportion of pre-symptomatic transmission	48%	38%	53%	Informed by viral load measurements, tracing results, and negative serial intervals described in (*5*, *27*, *33*, *39–44*)
% of symptomatic cases identified without tracing	90%			Assumes good health infrastructure
% of cases with chirping smartphones (high-uptake case)	80%			Assumes integration into all smartphones (*45*)
% of cases with chirping smartphones (low-uptake case)	53%			Survey data (*23*, *24*, *45*) with opt-in exposure event detection (*12*)
% of cases with smartphones who upload data when diagnosed	90%			Assumed (see Supplementary Methods)
% of cases who share data with manual contact tracers	98%			Non-cooperation reported to be rare (*46*)
Test sensitivity	80%			(*21*, *22*)
R_0 (default)	2.5			Most estimates cluster between 2.0 and 3.0: (*4*, *10*, *26–29*)
Overdispersion	0.11			(*47*)
Number of initial cases	20			Assumed
Data retention window for digital tracing (days)	14 days			(*12*)
Incubation period	5.5 ± 2.1 days (mean ± sd, lognormal distribution)			(*48*)
Delay from onset to isolation	3.8 ± 2.4 days (mean ± sd, Weibull distribution)			(*20*)
Delay for testing	1 ± 0.3 days (mean ± sd, gamma distribution)			Assumed
Delay for manual tracing	1.5 ± 4.8 days (mean ± sd, lognormal distribution); median 0.5 days			Previous reports suggest most contacts can be traced within one day, but some take much longer (*49*)
Delay for digital tracing	0 days			Assumed

Supplementary methods

1. Structure of the model - Infection dynamics

A new case is infected at some **exposure time**, equal to zero if the case is an index case and otherwise drawn from the **generation time distribution** of its parent case (see below). If not asymptomatic, the case develops symptoms at some **onset time** drawn from an **incubation time distribution**. Asymptomatic cases do not develop symptoms, but are still assigned an onset time for the purpose of determining their generation-time distribution (see below).

The number of child cases infected by the case is drawn from a negative binomial distribution, with mean equal to the appropriate reproduction number (see below) and heterogeneity determined by the overdispersion parameter k. The exposure times of these child cases are drawn from a skewed-normal **generation time distribution** centered on the symptom onset of their parent (*20*), with a skew parameter chosen to give a pre-specified probability of pre-symptomatic transmission (for a symptomatic parent). The generation time distribution for an asymptomatic parent is centered on its "effective" onset time (see above). The shape of the generation-time distribution is the same for all cases.

The average number of children produced by a case depends on its symptomatic status, and is determined by the overall R_0 value, the proportion of asymptomatic carriers p_{asym}, and the relative infectiousness x_{asym} of asymptomatic carriers (expressed as a fraction of R_0). Given a reproduction number for asymptomatics of $R_{asym} = R_0 \cdot x_{asym}$, the reproduction number of symptomatic cases that produces the desired overall R_0 is given by:

$$R_{sym} = R_{asym} \cdot \frac{p_{asym}}{1-p_{asym}}$$

2. Structure of the model - Infection control

Once symptoms develop, a case is **identified** by public health authorities with probability p_{isol}, with the delay from onset to identification drawn from a **delay distribution**. Identified cases are instructed to isolate, and each case complies with that order with probability p_{comply}. Cases that comply with isolation generate no further child cases after their time of identification. Asymptomatic cases cannot be identified from symptoms, but may be identified via contact tracing from other cases (see below); once identified, they are instructed to isolate as above. Tracing can also cause symptomatic cases to be isolated earlier than they would be from symptoms alone.

An identified case is **tested**, which takes time drawn from a test time distribution and returns a positive result with probability equal to the sensitivity of the test (since the model does not consider uninfected

individuals, the specificity of the test is also not considered). For asymptomatic cases, or symptomatic cases identified prior to symptom onset, a positive test result is required to initiate contact tracing; symptomatic cases that have already developed symptoms can either be traced immediately upon identification, or require a positive test result prior to tracing, depending on model settings.

Whether before or after a test result is obtained, the contacts of an identified case can also be **traced**. Tracing can only proceed outward from a case if they share their contact history, either via a contact-tracing app or with a manual contact tracer (see below). Tracing can identify the children of the traced case (forward tracing), and may also be able to identify its parent (reverse/backward tracing), depending on model settings. The speed and success probability of tracing depend upon whether tracing is conducted digitally or manually, which in turn depends on several factors:

- If the contact between the trace originator and the tracee occurred environmentally (determined with probability p_{env}), tracing cannot take place.
- If transmission was not environmental, the contact can be traced digitally if:
    - Both the trace originator and the tracee possess chirp-enabled smartphones (determined independently for each individual case with probability $p_{smartphone}$);
    - The trace originator shares their data with the tracing app (determined independently for each individual case with probability $p_{share_digital}$);
    - The time of between contact (equal to the exposure time of the child case, i.e. of the trace in forward tracing and the trace initiator in reverse tracing) and trace initiation is less than the **data-retention window** of the digital tracing system;
    - The contact between the two cases was recorded by the tracing app of the trace originator (determined independently for each individual case with probability $p_{trace_digital}$).
- If any of the above conditions are not met, but transmission was not environmental, the contact might still be traced manually if:
    - The trace originator shares their contact history with a manual contact tracer (determined independently for each individual case with probability p_{share_manual});
    - The time between contact (as above) and the identification time or symptom onset of the trace initiator (whichever came first) is less than the **contact-tracing window** of the manual tracing system;
    - The tracee is successfully traced by the contact tracer (determined independently for each individual case with probability p_{trace_manual}).
- If neither digital nor manual tracing succeeds, then the trace fails and the tracee is not traced.

Cases that are successfully traced are identified at a time equal to the **trace initiation time** of the trace originator plus a delay time drawn from the appropriate **trace delay distribution** (which will differ between digital and manual tracing). Cases identified through tracing can then be isolated, tested, and traced as

described above. If a case is isolated through tracing earlier than they would have been otherwise, child cases whose exposure time would be later than their parent's new isolation time are eliminated, as are their descendents.

3. Run initiation and termination

A simulation of an outbreak under the branching-process model is initialised with a given number of index cases (by default 20) and proceeds generation by generation until either no further child cases are generated (extinction) or the run exceeds one of:

1. A **cumulative case limit** of 10,000 cases, reached if the total number of cases ever exceeded that number, or
2. A **time limit** of 52 weeks, reached if the latest exposure time across all cases ever exceeded that number.

In practice, virtually all runs either went extinct or reached the cumulative case limit; across all scenarios tested for all datasets used in Figures 2-4, the overall percentage of runs that terminated as a result of exceeding the time limit was less than 0.02%, and the highest percentage observed for any single scenario was 1.3%. The cumulative case limit, meanwhile, was selected to minimise the chance of a run that would otherwise go extinct being terminated prematurely while preserving computational tractability; in test runs with a cumulative case limit of 100,000 cases, fewer than 2% of extinct runs in any scenario had a cumulative case count of over 10,000.

A terminated run was deemed "controlled" if it reached extinction, and uncontrolled otherwise. The control rate for a scenario was computed as the proportion of runs for that scenario that were controlled. 95% credible intervals on the control rate were computed by beta-binomial conjugacy under a $Beta(1,1)$ uniform prior, as the 2.5th and 97.5th percentiles of the beta distribution $Beta(1+k, 1+n-k)$, where n is the total number of runs for that scenario and $k$is the number of controlled runs. Effective reproduction numbers were computed as the average number of child cases produced across all cases in a run, averaged across all runs in the scenario.

Supplementary Figures

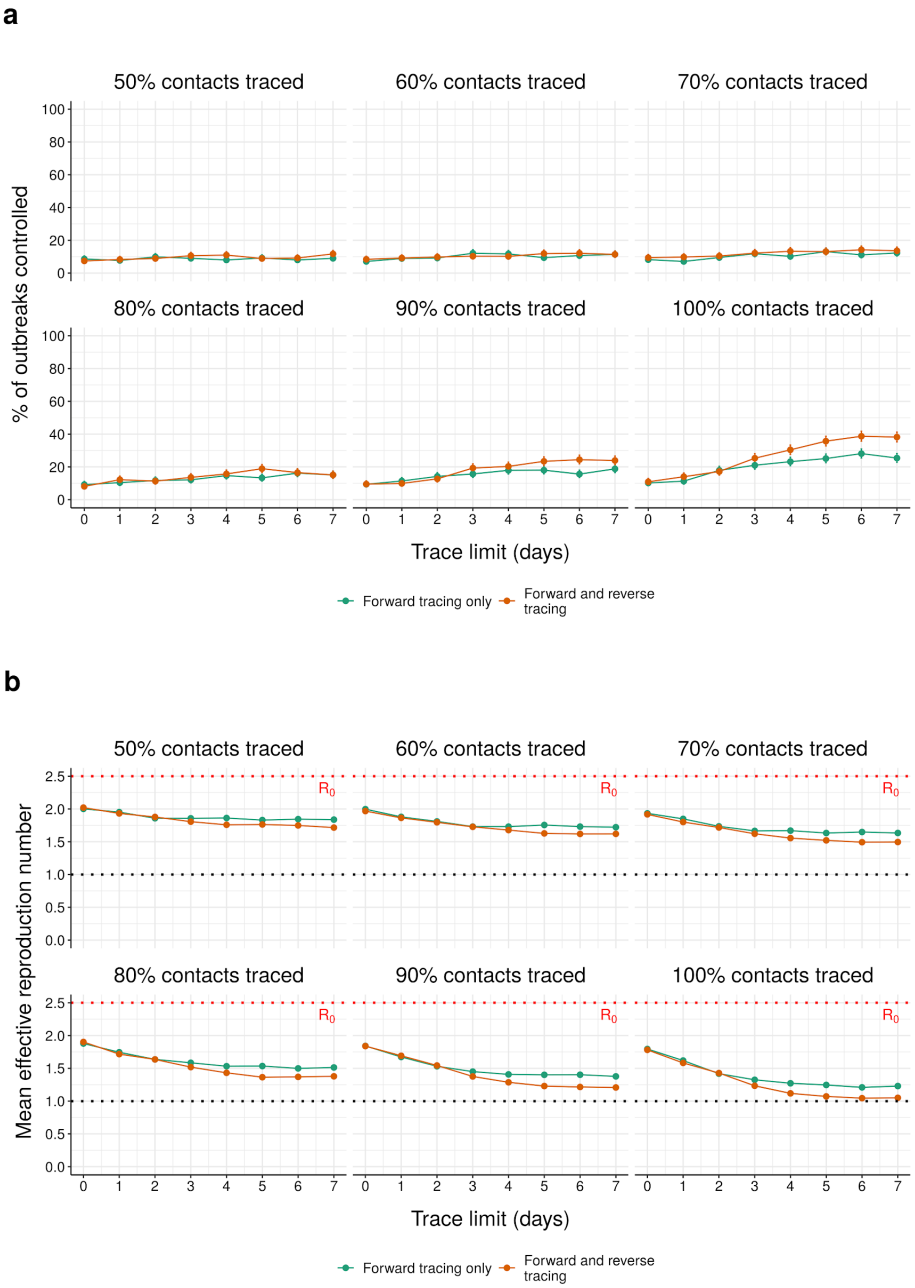

Figure S1: Effect of contact-tracing window size on performance of manual tracing. (a) Control rate and (b) average effective reproduction number of manual tracing under median parameters (Table 1) when contacts are traced for varying periods prior to symptom onset (for symptomatic cases) or case identification (for presymptomatic and asymptomatic cases). Panel headers indicate the percentage of non-environmental contacts traced. Error bars in (a) represent 95% credible intervals across 1000 runs; points in (b) represent average values over the same.

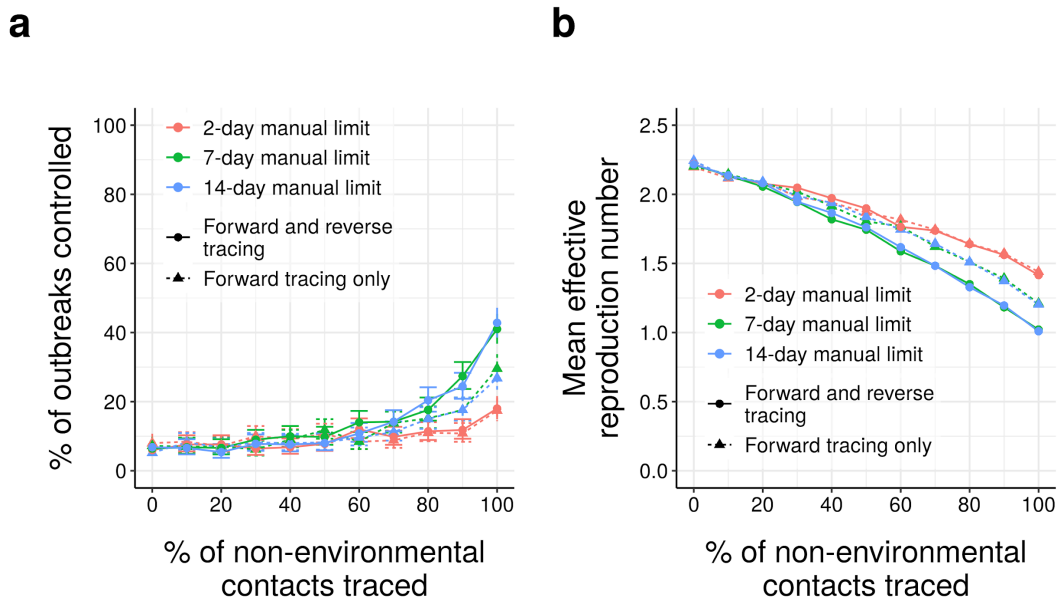

Figure S2: Effect of increased contact-tracing window size on performance of manual tracing. (a) Control rate and (b) average effective reproduction number of manual tracing under median parameters (Table 1) when contacts are traced up to 2, 7, or 14 days prior to symptom onset (for symptomatic cases) or case identification (for presymptomatic and asymptomatic cases). Error bars in (a) represent 95% credible intervals across 500 runs; points in (b) represent average values over the same.

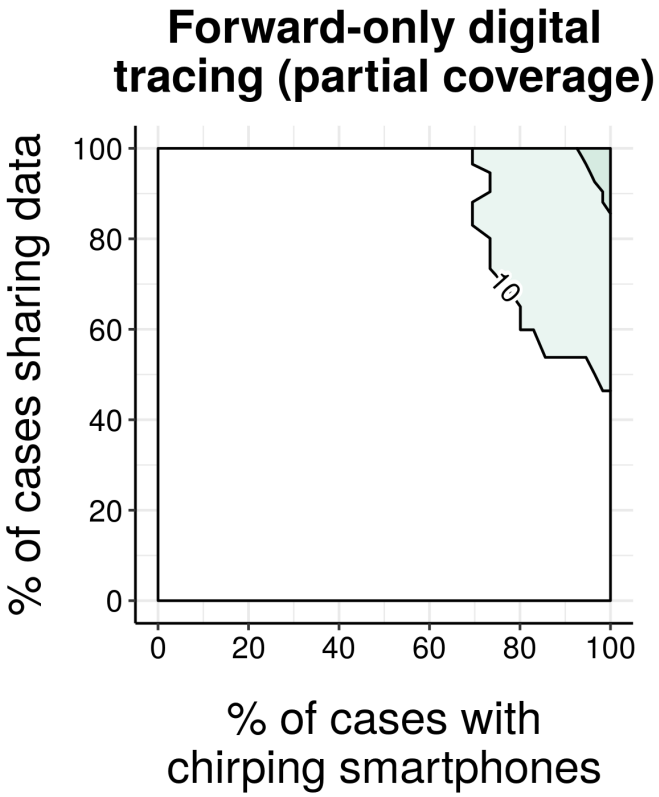

Figure S3: Effect of network fragmentation on performance of forward-only digital tracing. Smoothed contour plot of % outbreaks controlled over 1000 runs per scenario, assuming median disease parameters (Table 1) and that 90% of non-environmental contacts that can be traced digitally are traced successfully.

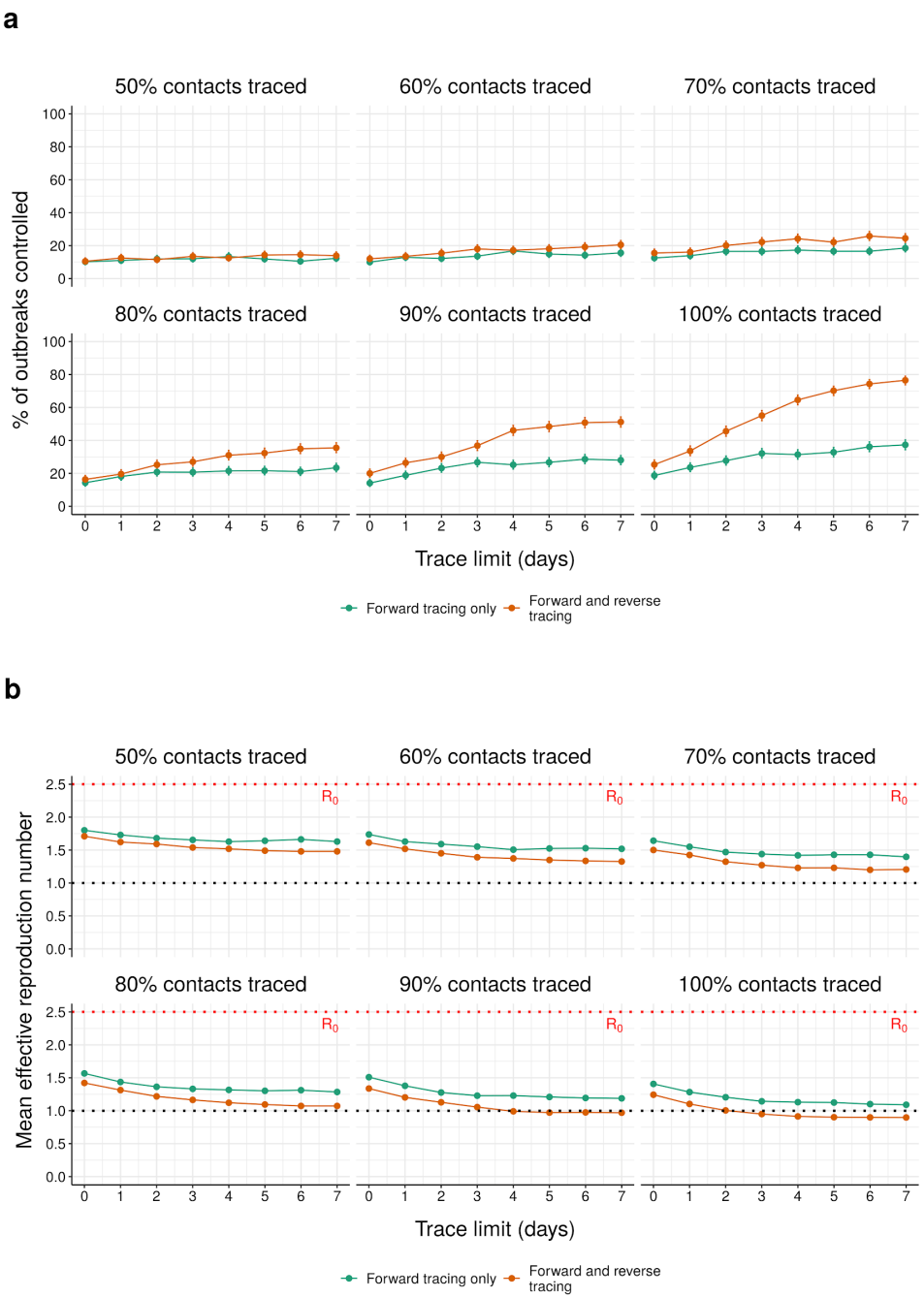

Figure S4: Effect of contact-tracing window size on performance of combined tracing. (a) Control rate and (b) average effective reproduction number of combined manual and digital tracing under median parameters (Table 1) when contacts are manually traced for varying periods prior to symptom onset (for symptomatic cases) or case identification (for presymptomatic and asymptomatic cases). Data for digital contact tracing is assumed to be retained for 14 days after contact. Panel headers indicate the percentage of non-environmental contacts traced. Error bars in (a) represent 95% credible intervals across 1000 runs; points in (b) represent average values over the same.

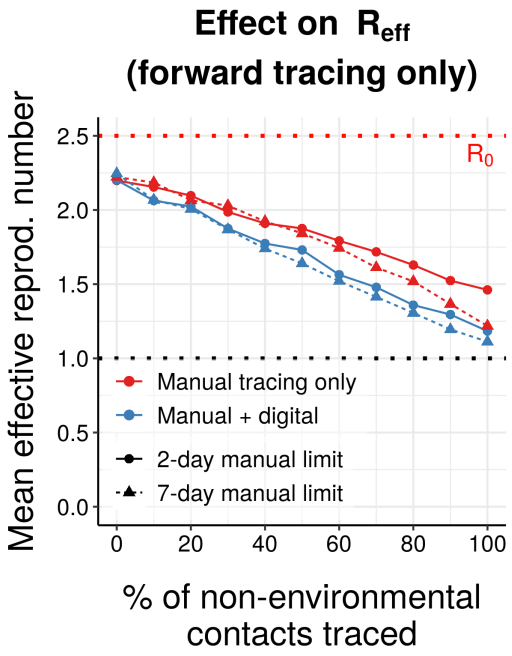

Figure S5: Effective reproduction numbers under forward-only tracing. As Fig. 3e, but with forward only rather than bidirectional tracing. Points represent average values over 1000 runs.

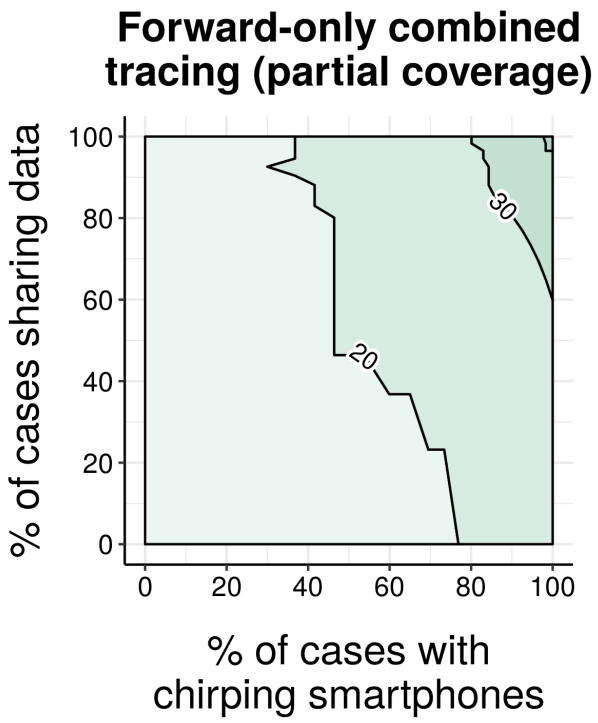

Figure S6: Effect of network fragmentation on performance of forward-only combined (manual + digital) tracing. Smoothed contour plot of % outbreaks controlled over 1000 runs per scenario, assuming median disease parameters (Table 1) and that 90% of non-environmental contacts that can be traced digitally are traced successfully.

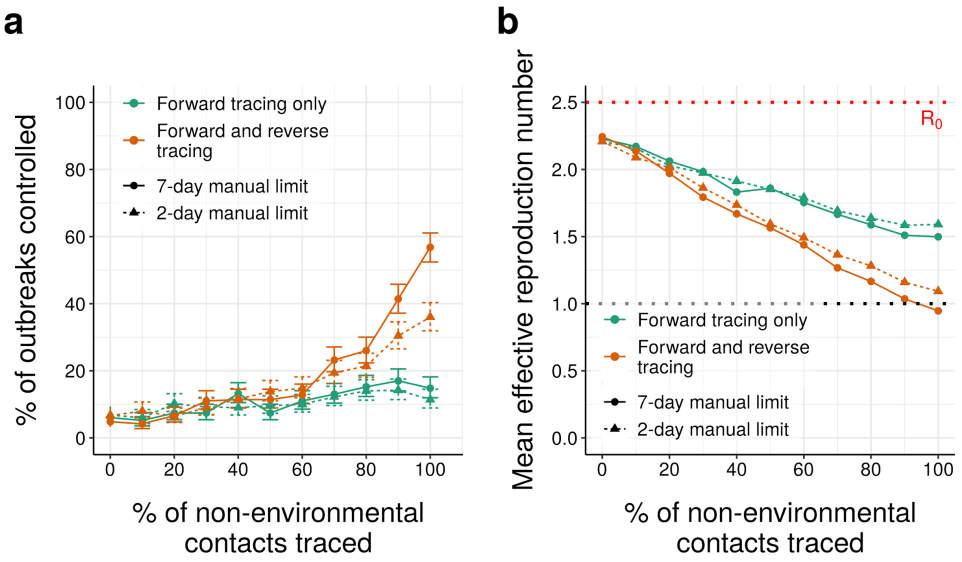

Figure S7: Effect of requiring pre-trace testing on combined trace performance. As Fig. 3e-f, but requiring a positive test result before initiating contact tracing from a symptomatic case. Error bars in (a) represent 95% credible intervals across 500 runs; points in (b) represent average values over the same.

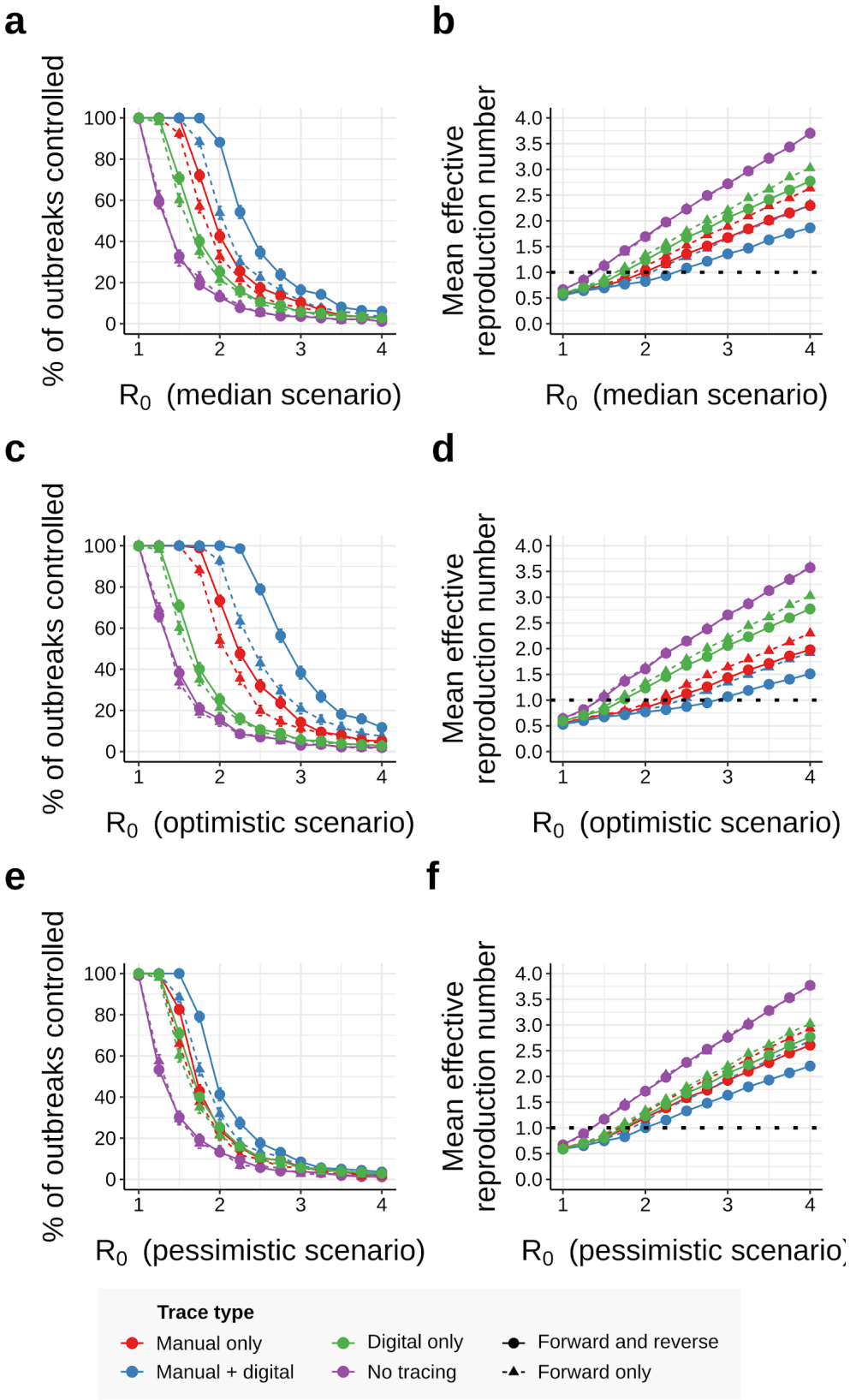

Figure S8: Effect of R_0 and disease parameters on tracing performance (80% trace rate). As Figure 3, but assuming 80% of non-environmental contacts are traced.

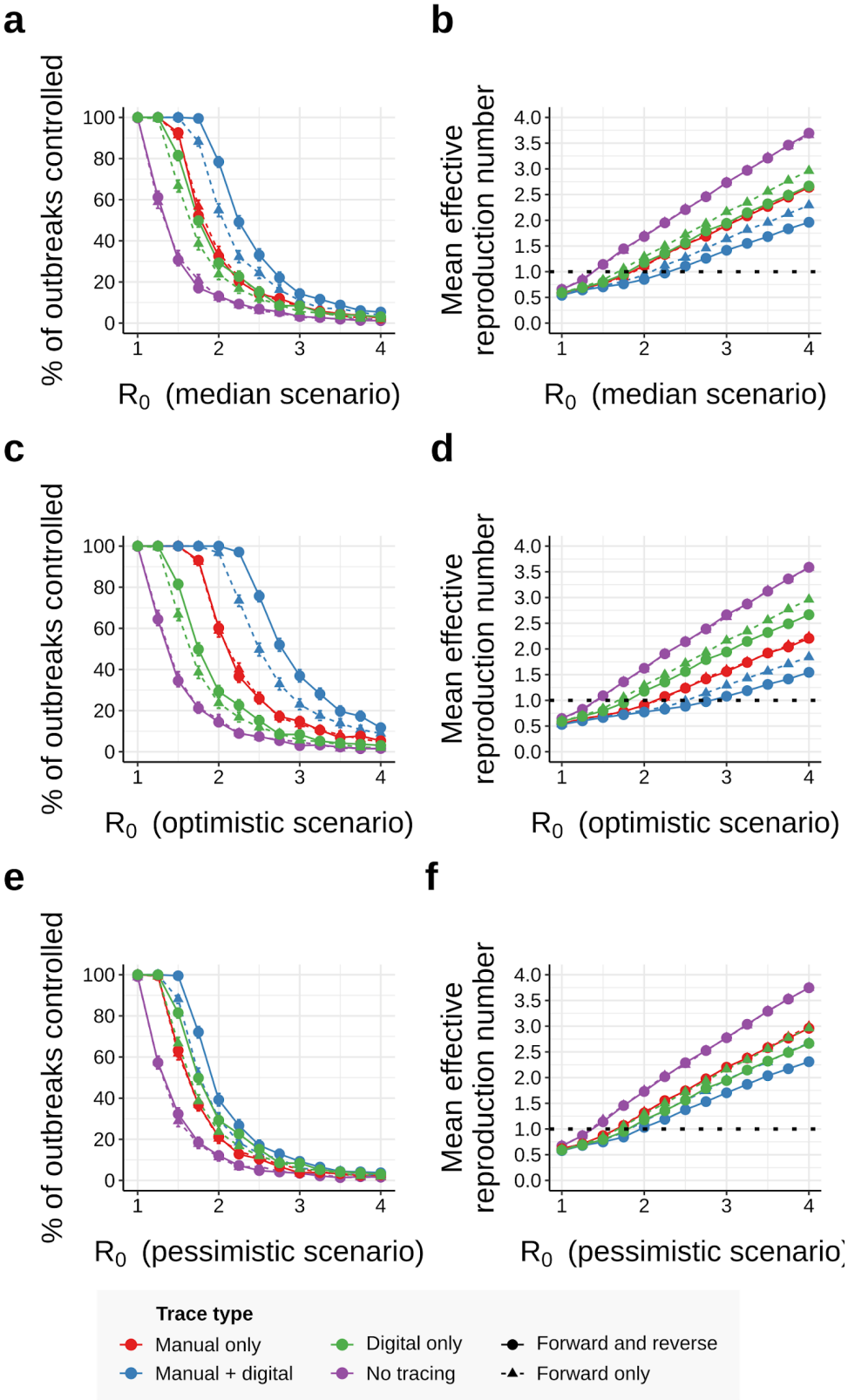

Figure S9: Effect of R_0 and disease parameters on tracing performance (2-day manual trace window). As Figure 3, but assuming a 2-day manual trace window.

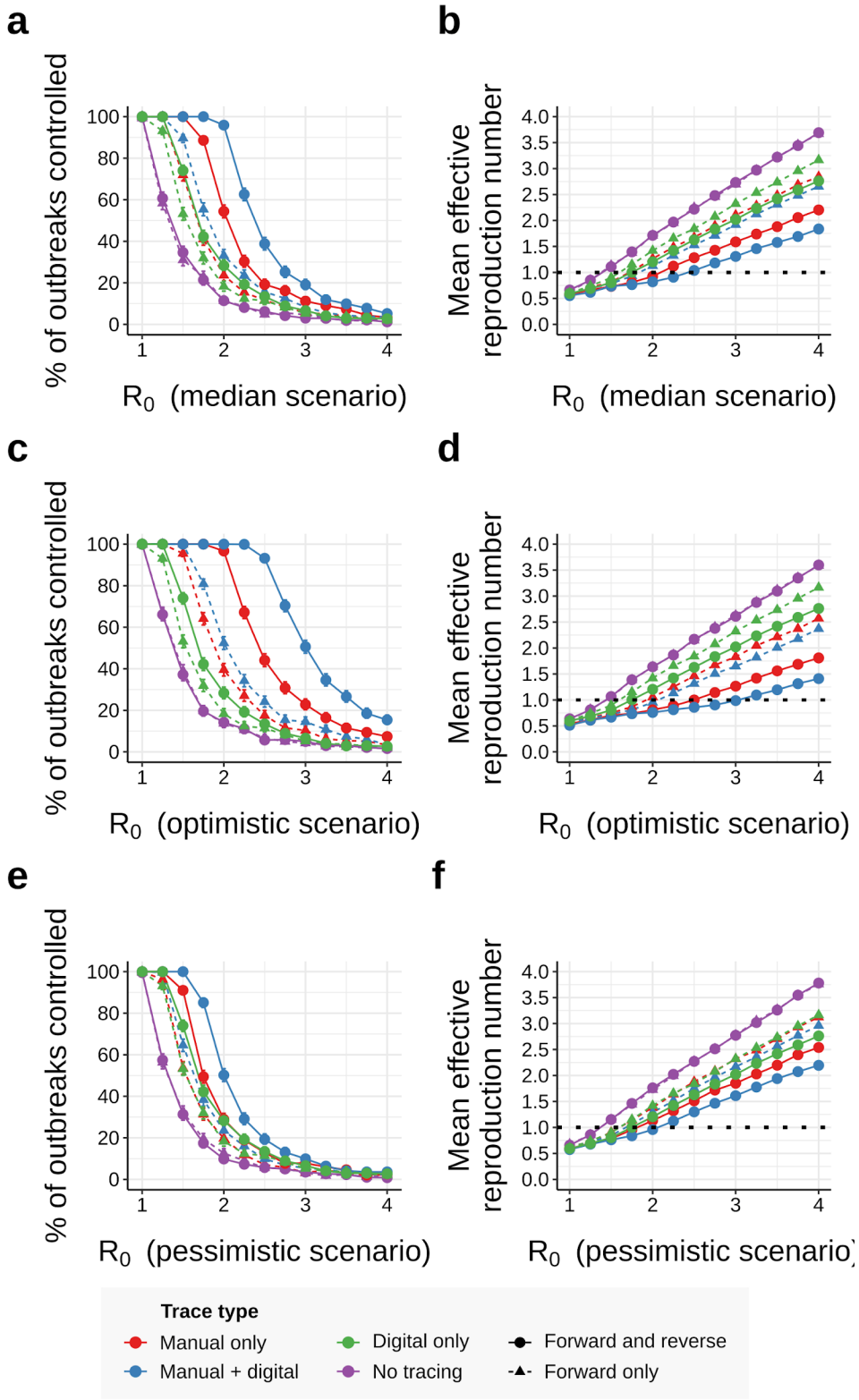

Figure S10: Effect of R_0 and disease parameters on tracing performance (pre-emptive testing). As Figure 3, but requiring a positive test result before tracing symptomatic cases.

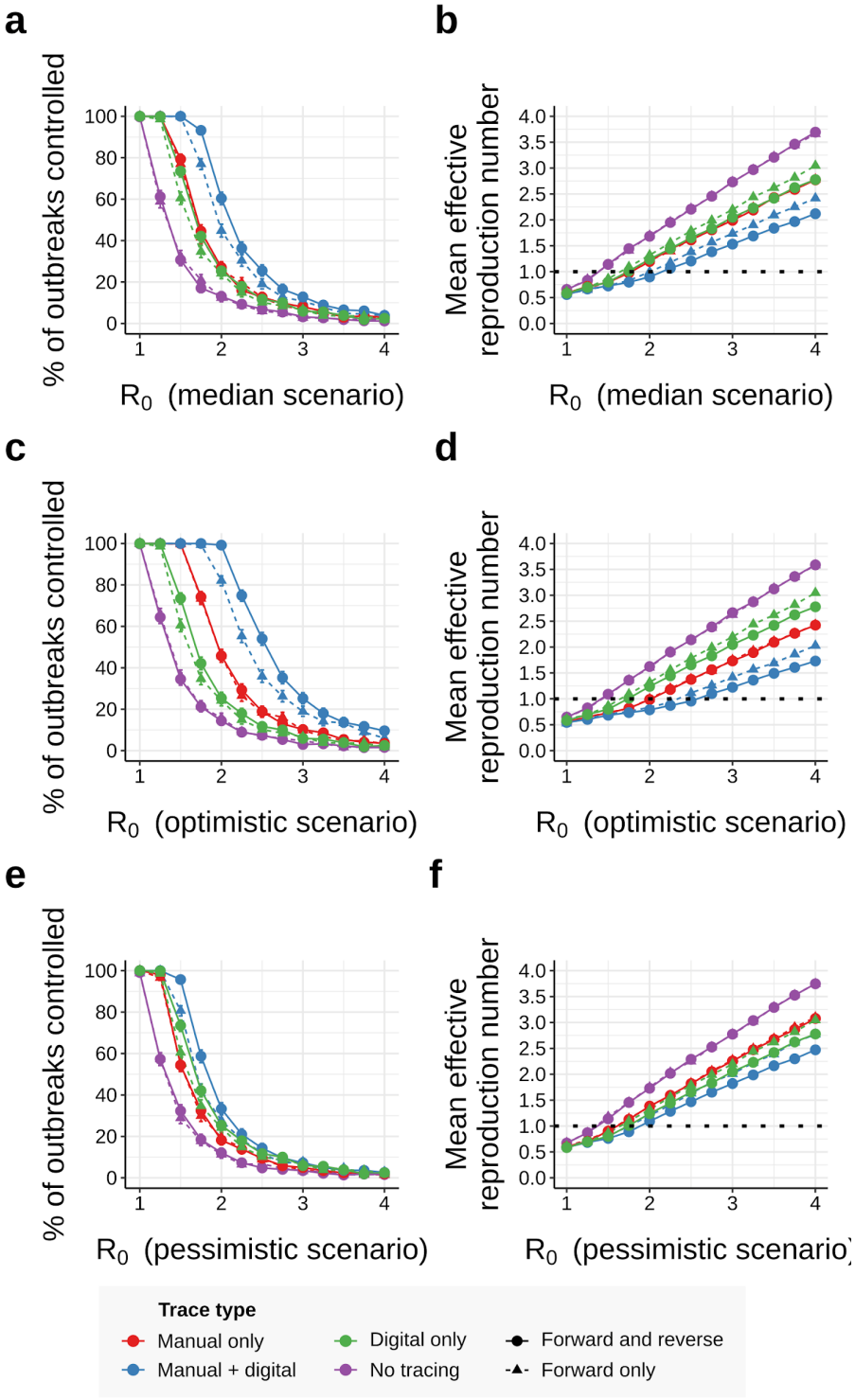

Figure S11: Effect of R_0 and disease parameters on tracing performance (80% trace rate, 2-day manual trace window). As Figure 3, but assuming 80% of non-environmental contacts traced and a 2-day manual trace window.

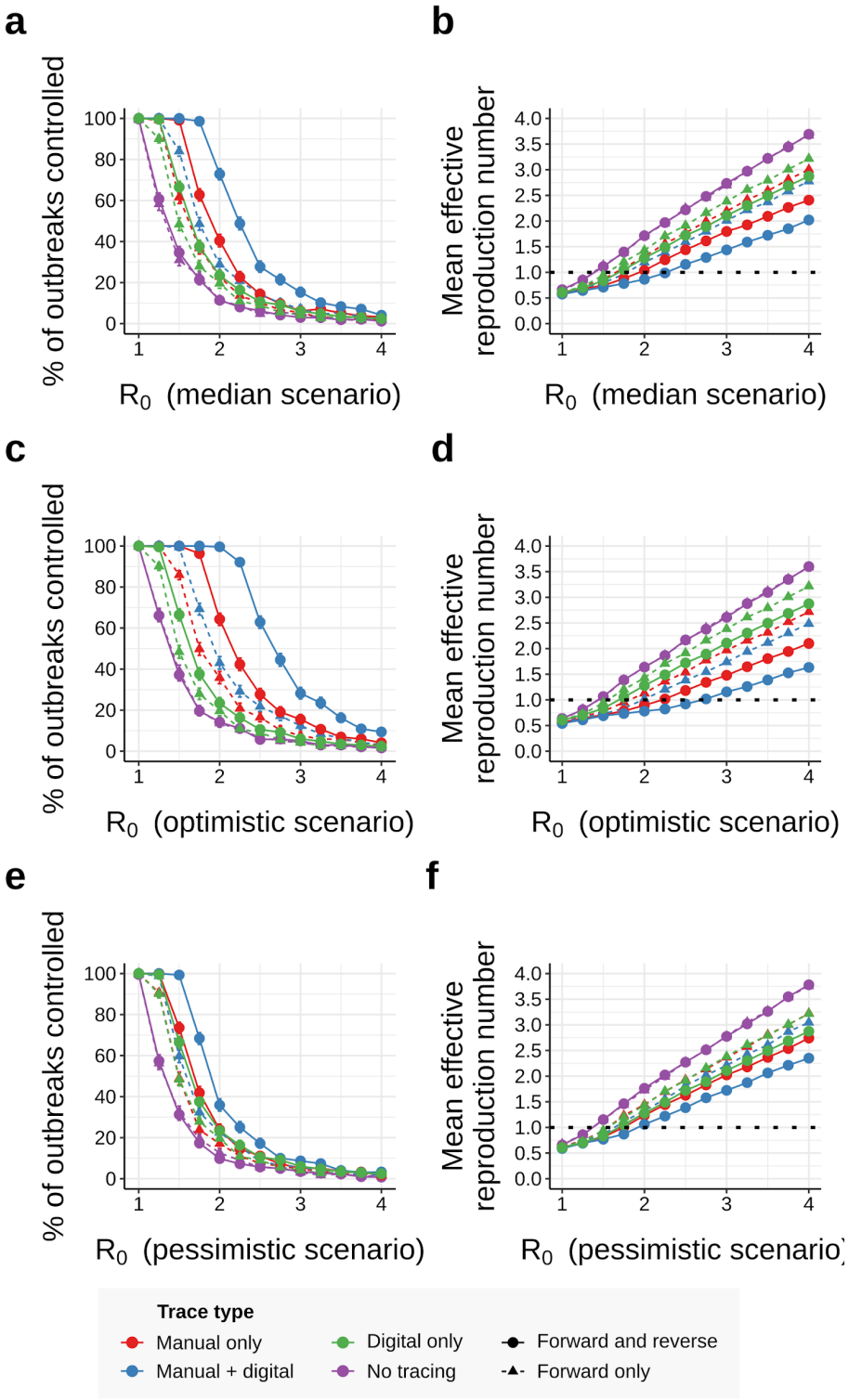

Figure S12: Effect of R_0 and disease parameters on tracing performance (pre-emptive testing, 80% trace rate). As Figure 3, but requiring a positive test result before tracing symptomatic cases and assuming 80% of non-environmental contacts traced and a 2-day manual trace window.

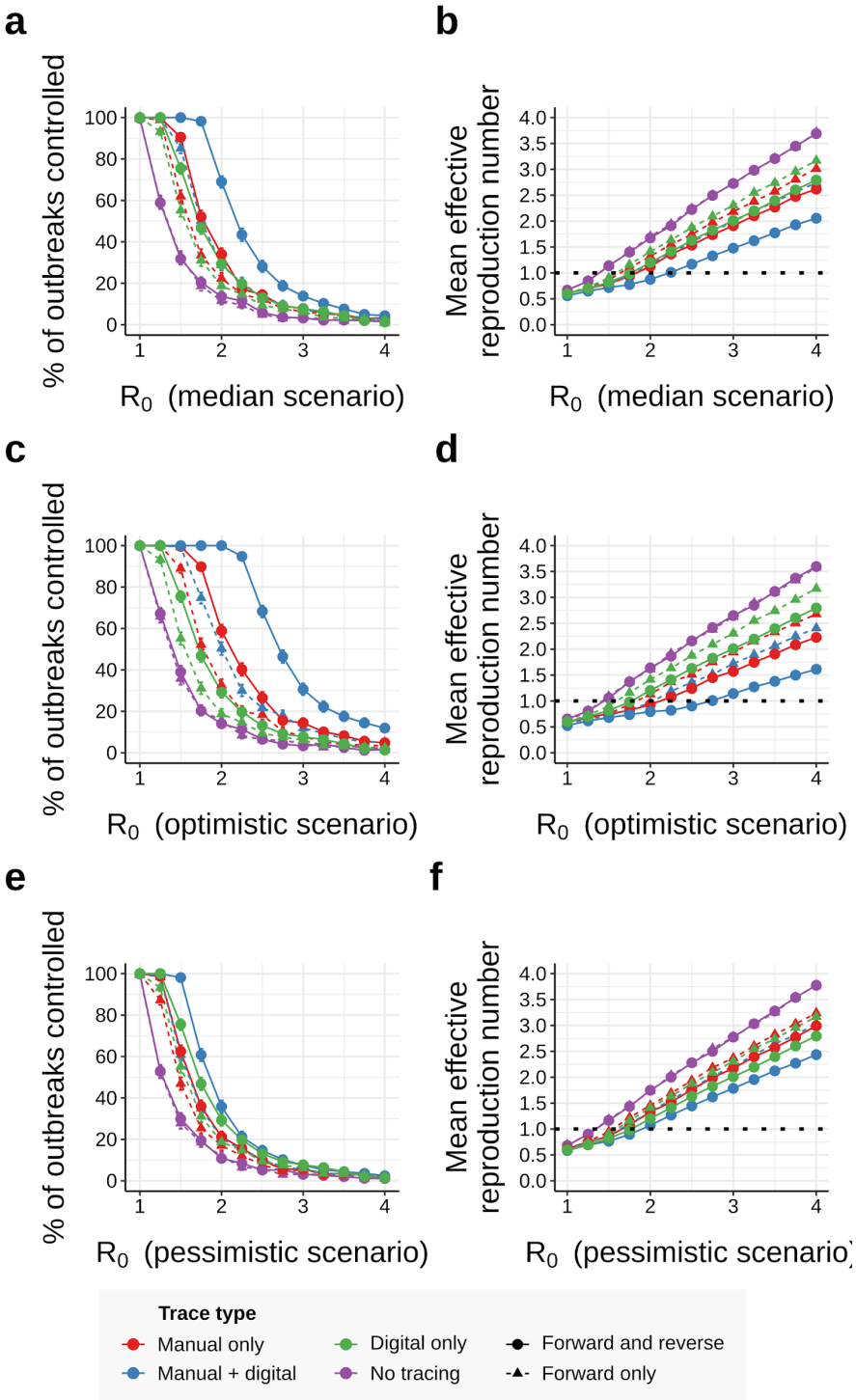

Figure S13: Effect of R_0 and disease parameters on tracing performance (pre-emptive testing, 2-day manual trace window). As Figure 3, but requiring a positive test result before tracing symptomatic cases and assuming a 2-day manual trace window.

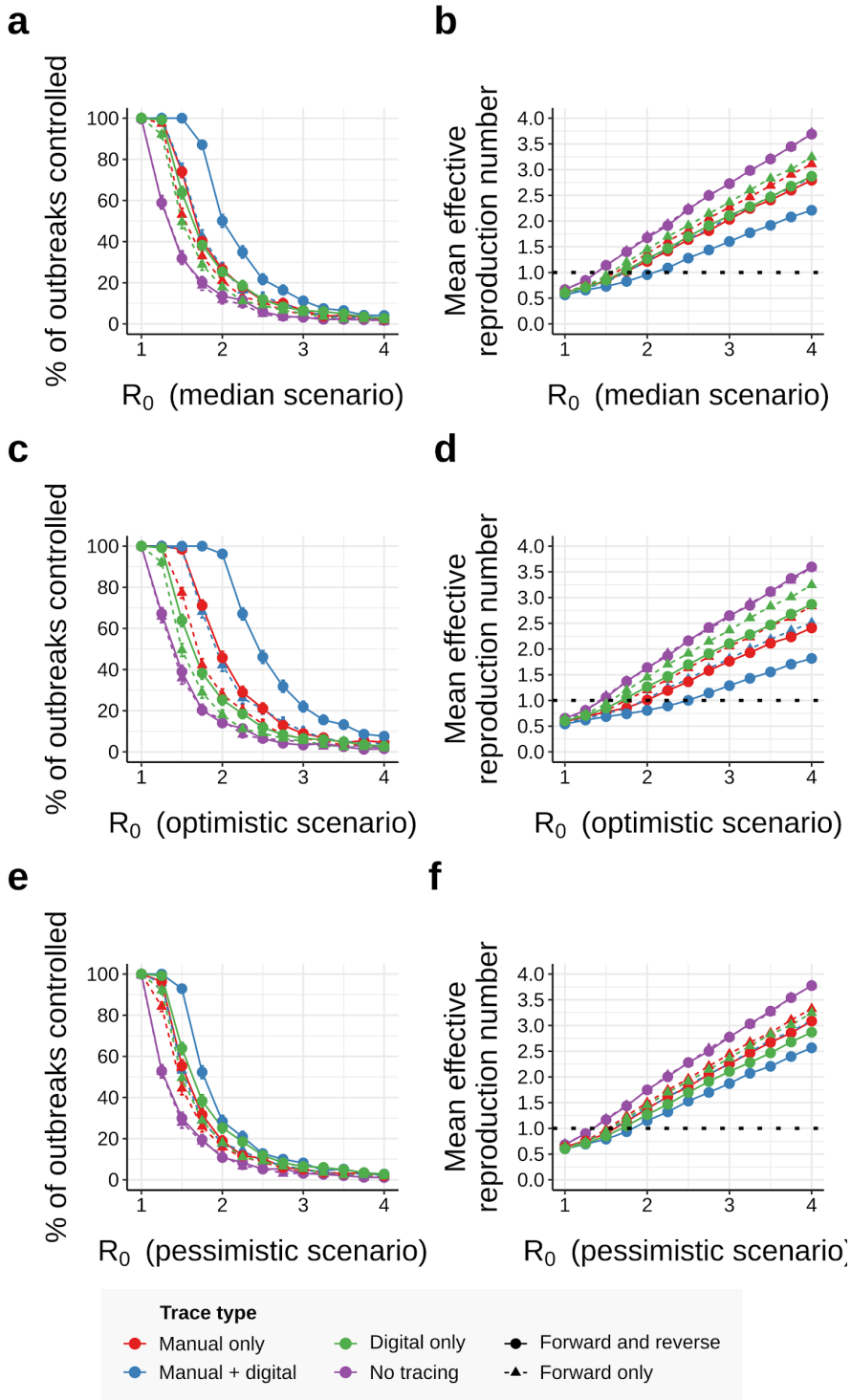

Figure S14: Effect of R_0 and disease parameters on tracing performance (pre-emptive testing, 80% trace rate, 2-day manual trace window). As Figure 3, but requiring a positive test result before tracing symptomatic cases, and assuming 80% of non-environmental contacts traced and a 2-day manual trace window.

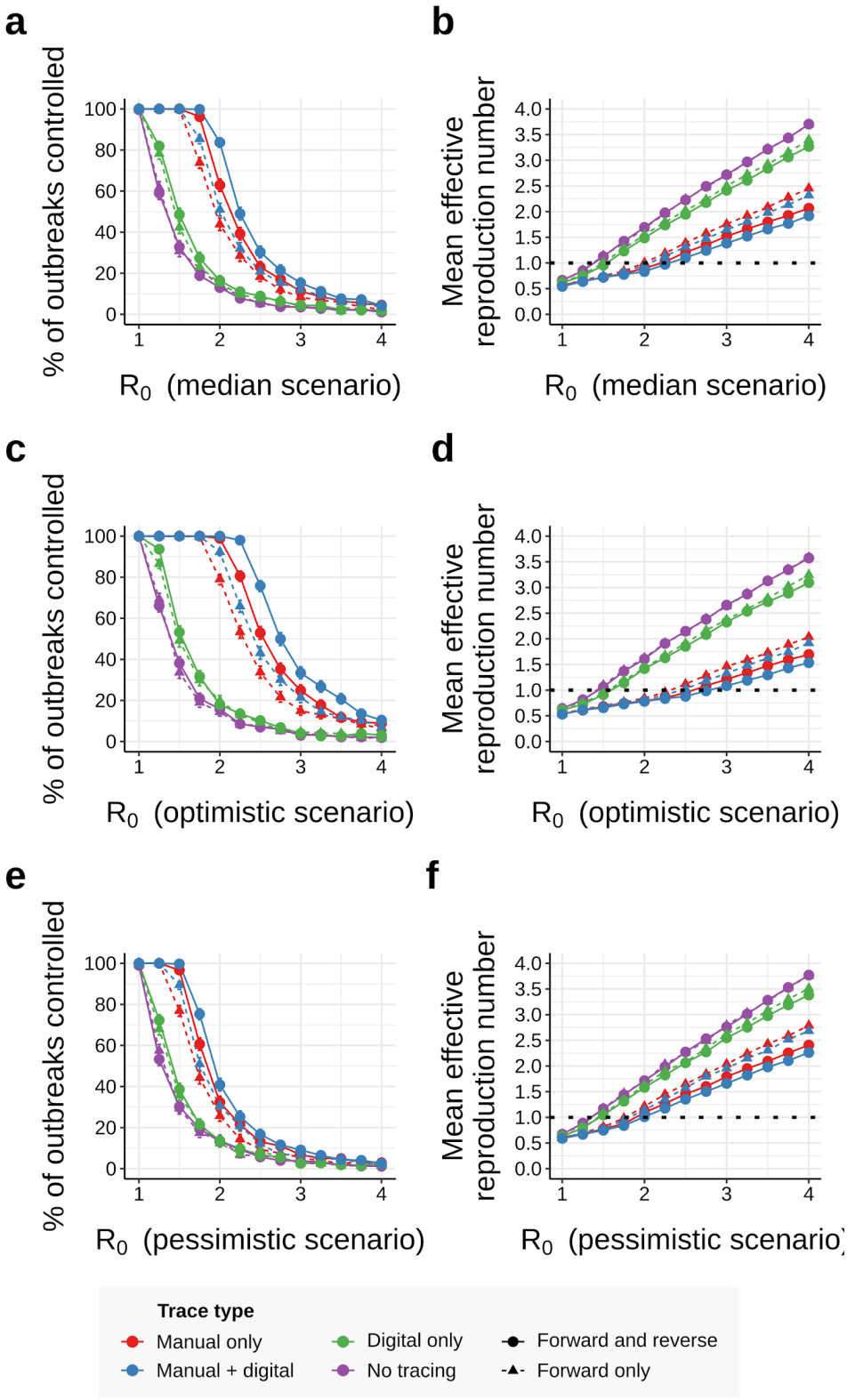

Figure S15: Effect of R_0 and disease parameters on tracing performance (low-uptake case). As Figure 3, but assuming only 53% of cases have chirp-enabled smartphones.

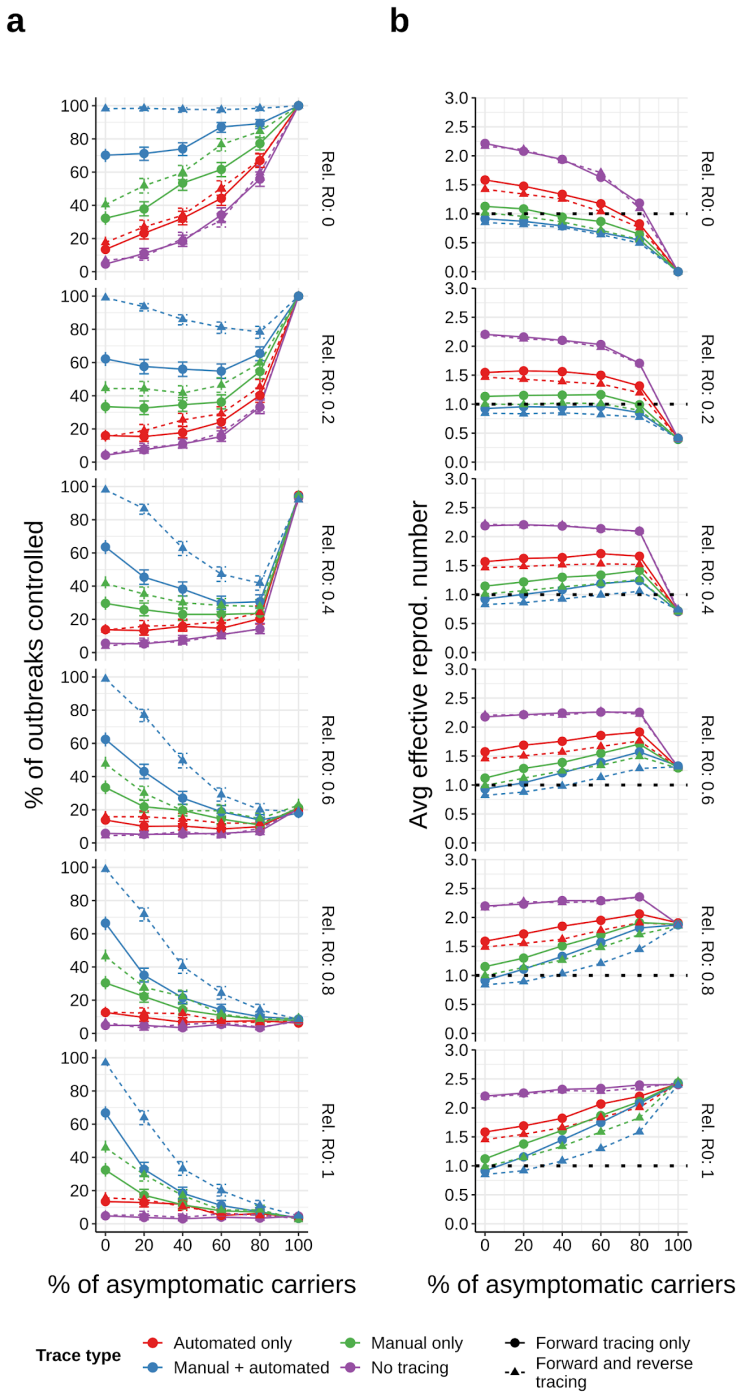

Figure S16: Effect of the rate and infectiousness of asymptomatic carriers on epidemic control. (a) Control rates and (b) Average effective reproduction number achieved under different combinations of the rate (%) and relative infectiousness ("Rel. R0") of asymptomatic carriers, assuming otherwise median disease parameters (Table 1), 90% of non-environmental contacts traced and a 7-day manual trace window. Error bars in (a) represent 95% credible intervals across 500 runs; points in (b) represent average values over the same.

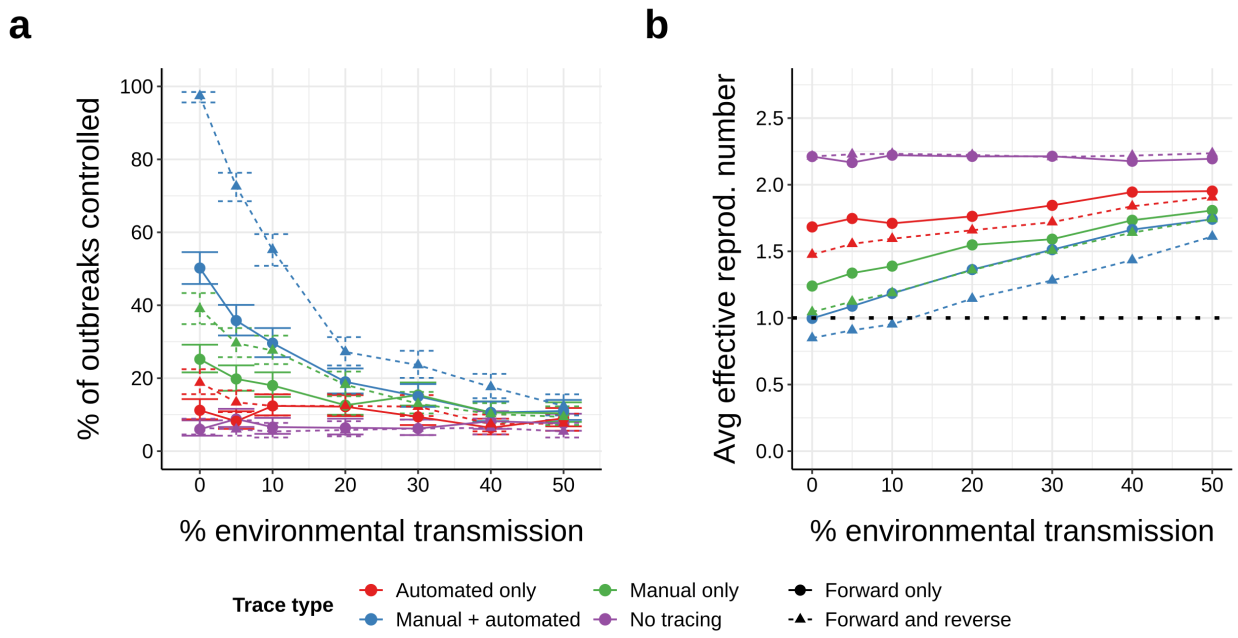

Figure S17: Effect of environmental transmission on epidemic control. (a) Control rates and (b) Average effective reproduction numbers achieved under different rates of environmental transmission, assuming otherwise median disease parameters (Table 1), 90% of non-environmental contacts traced and a 7-day manual trace window. Environmental transmission is assumed to be untraceable by either manual or digital contact tracing. Error bars in (a) represent 95% credible intervals across 500 runs; points in (b) represent average values over the same.

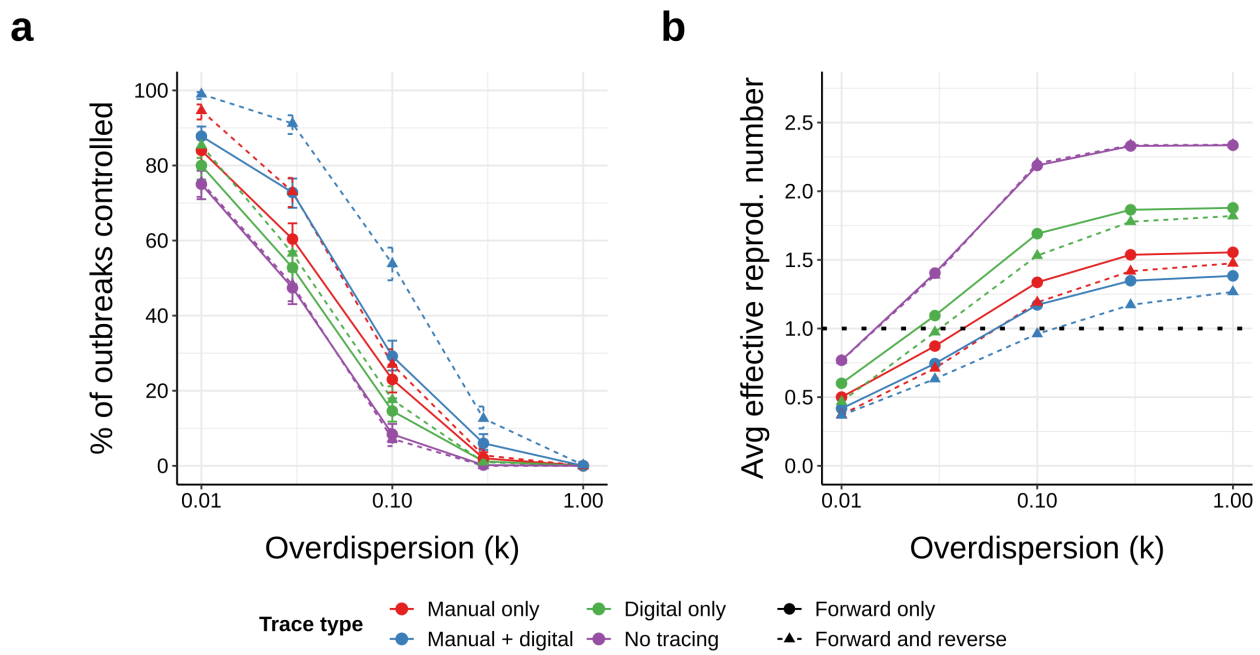

Figure S18: Effect of overdispersion parameter on epidemic control. (a) Control rates and (b) Average effective reproduction numbers achieved under different values of the overdispersion parameter *k* (where lower values of *k* denote higher variance in infectiousness among cases), assuming otherwise median disease parameters (Table 1), 90% of non-environmental contacts traced and a 7-day manual trace window. Error bars in (a) represent 95% credible intervals across 500 runs; points in (b) represent average values over the same.

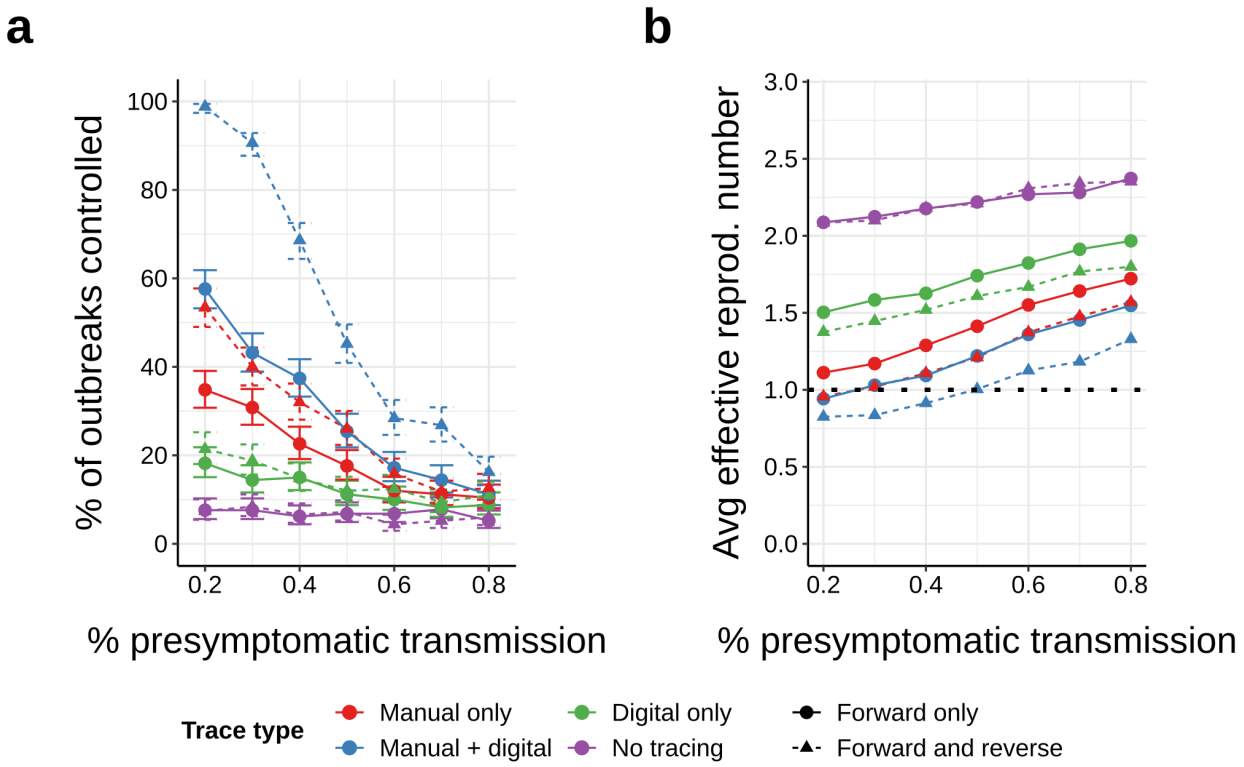

Figure S19: Effect of pre-symptomatic transmission on epidemic control. (a) Control rates and (b) Average effective reproduction numbers achieved under different rates of pre-symptomatic transmission, assuming otherwise median disease parameters (Table 1), 90% of non-environmental contacts traced and a 7-day manual trace window. Error bars in (a) represent 95% credible intervals across 500 runs; points in (b) represent average values over the same.

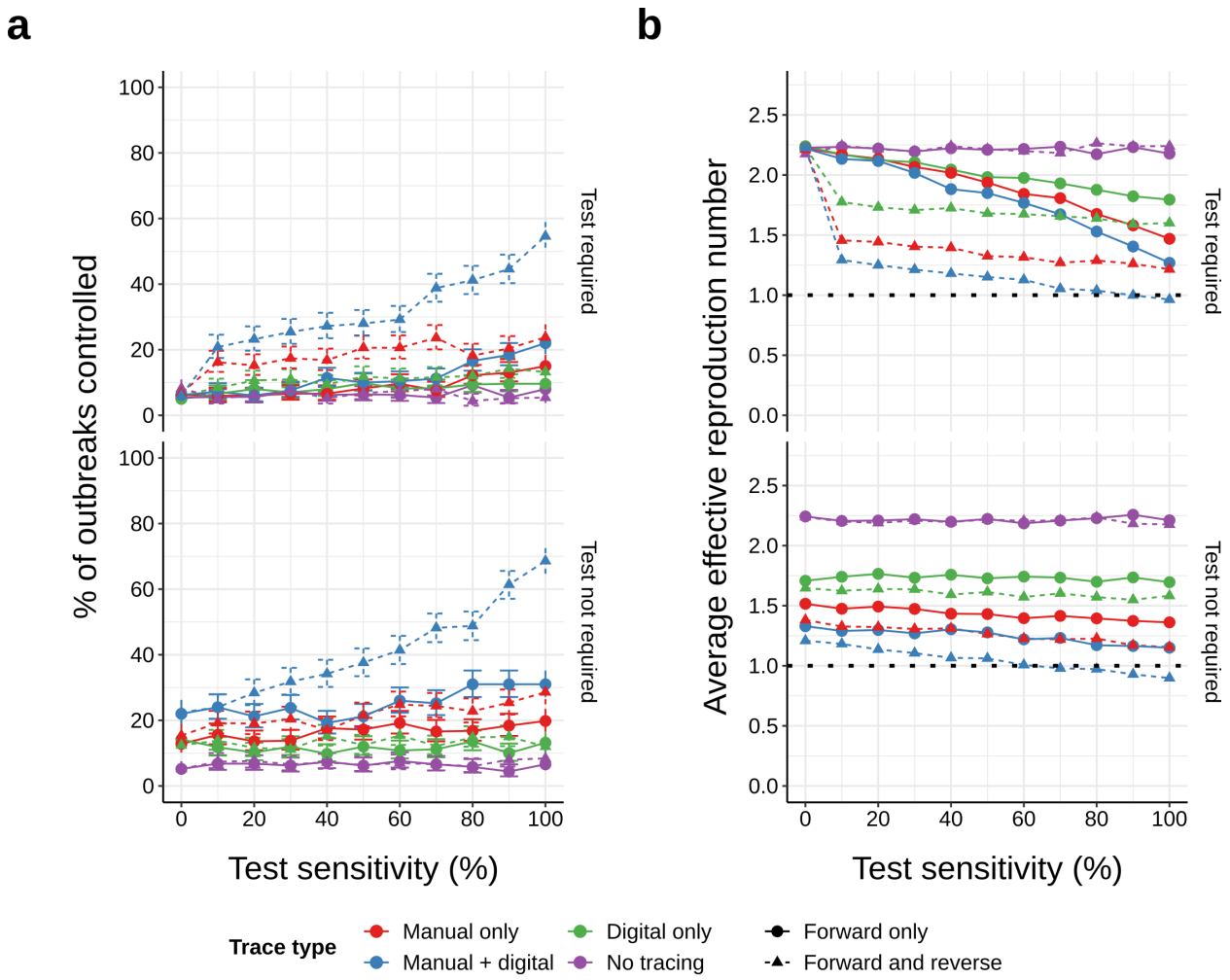

Figure S20: Effect of test sensitivity on epidemic control. (a) Control rates and (b) Average effective reproduction numbers achieved under different assumptions about test sensitivity (x-axis) and whether or not a positive test result is required before contact tracing from a symptomatic case (top/bottom panels) , assuming otherwise median disease parameters (Table 1), 90% of non-environmental contacts traced and a 7-day manual trace window. Error bars in (a) represent 95% credible intervals across 500 runs; points in (b) represent average values over the same.

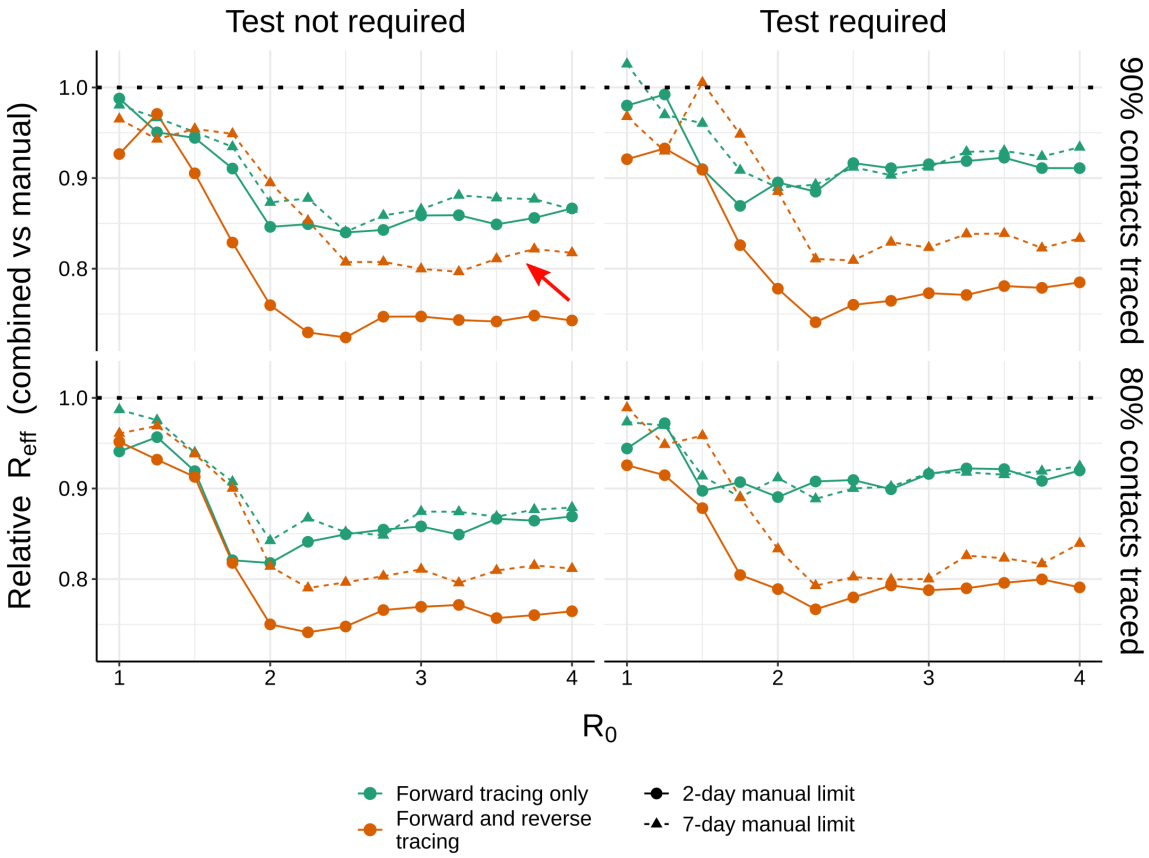

Figure S21: Relative effective reproduction number of manual and combined tracing. Ratio between the effective reproduction number achieved by combined tracing and that achieved by manual-only tracing under median disease parameters (Table 1), in the presence or absence of bidirectional tracing and for different rates of non-environmental contacts traced, manual tracing windows, and pre-trace testing policies for symptomatic cases. The red arrow indicates the curve corresponding to Figure 4b.

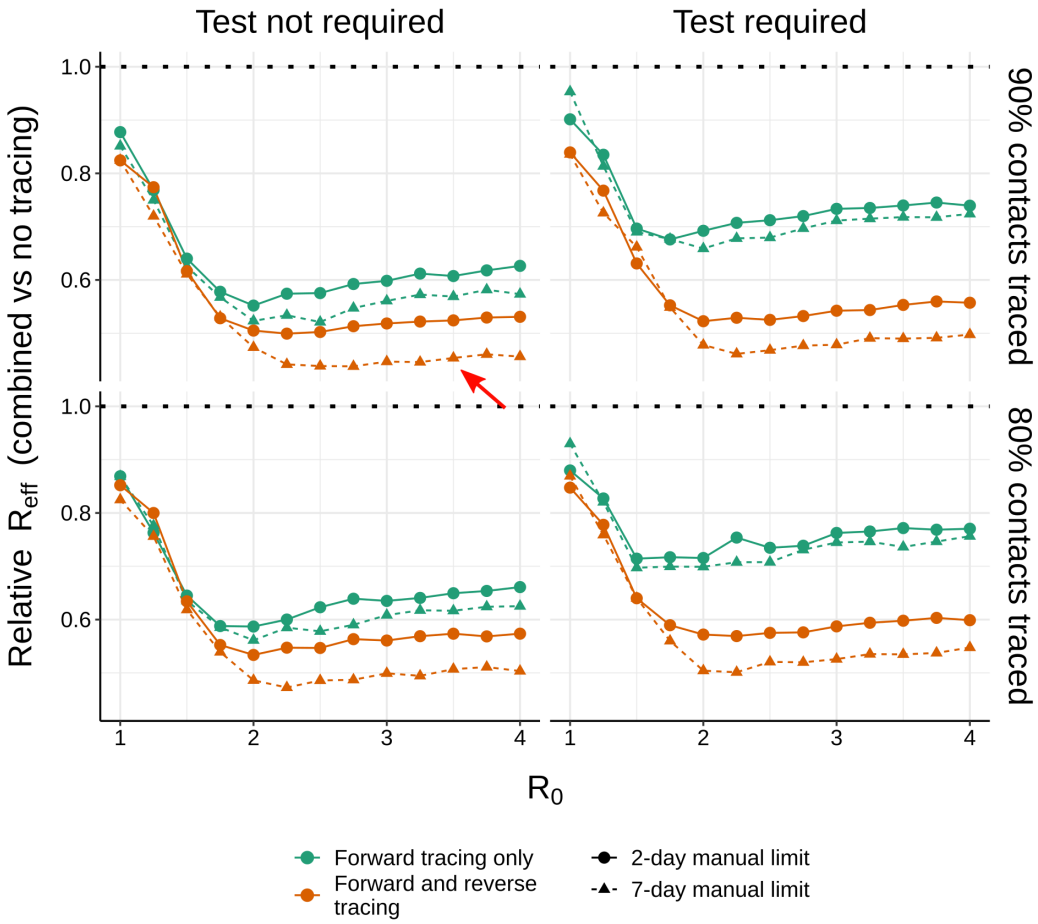

Figure S22: Relative effective reproduction number of combined vs no tracing. Ratio between the effective reproduction number achieved by combined tracing and that achieved without contact tracing (i.e. solely under isolation of symptomatic cases) under median disease parameters (Table 1), in the presence or absence of bidirectional tracing and for different rates of non-environmental contacts traced, manual tracing windows, and pre-trace testing policies for symptomatic cases. The red arrow indicates the curve corresponding to Figure 4b.

a

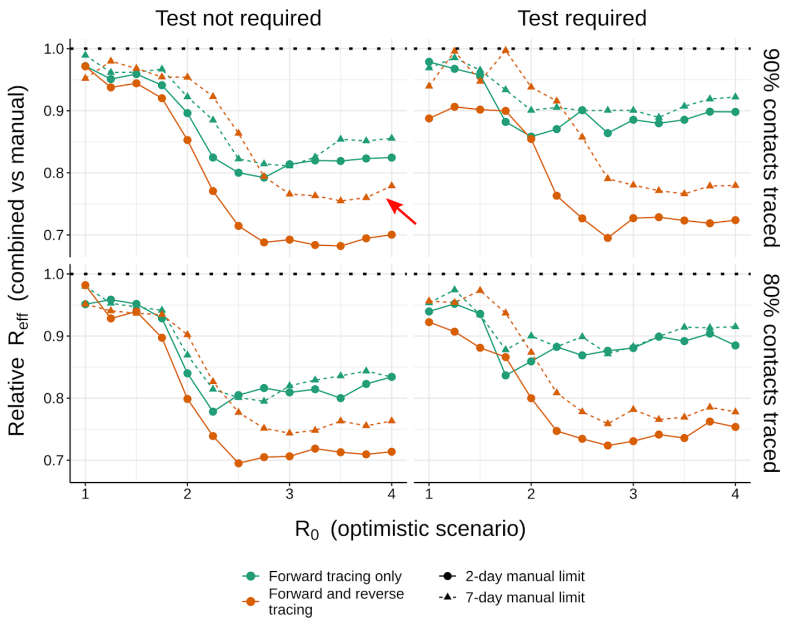

b

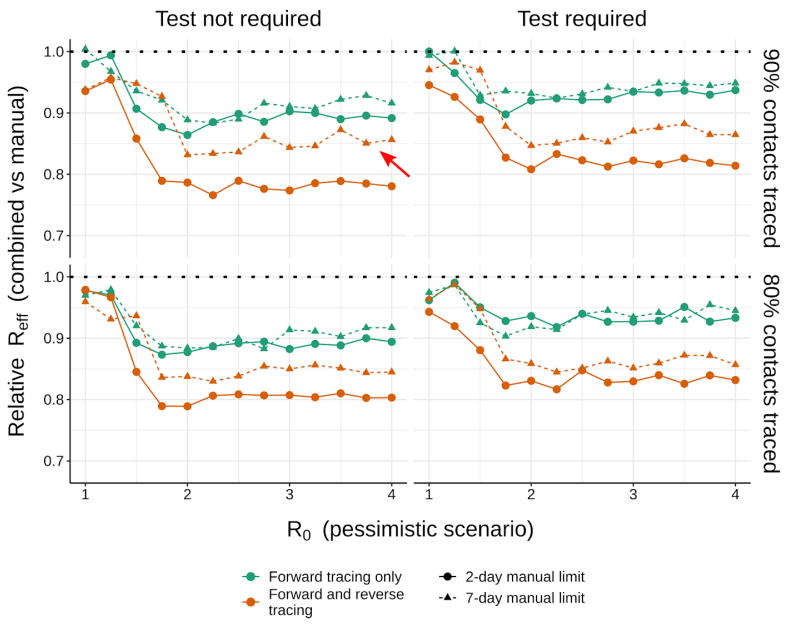

Figure S23: Relative effective reproduction number of manual and combined tracing (optimistic and pessimistic scenarios). Ratio between the effective reproduction number achieved by combined tracing and that achieved by manual-only tracing under (a) optimistic and (b) pessimistic disease parameters (Table 1), in the presence or absence of bidirectional tracing and for different rates of non-environmental contacts traced, manual tracing windows, and pre-trace testing policies for symptomatic cases. The red arrows indicate the curves corresponding to Figures 5b and 5d.

a

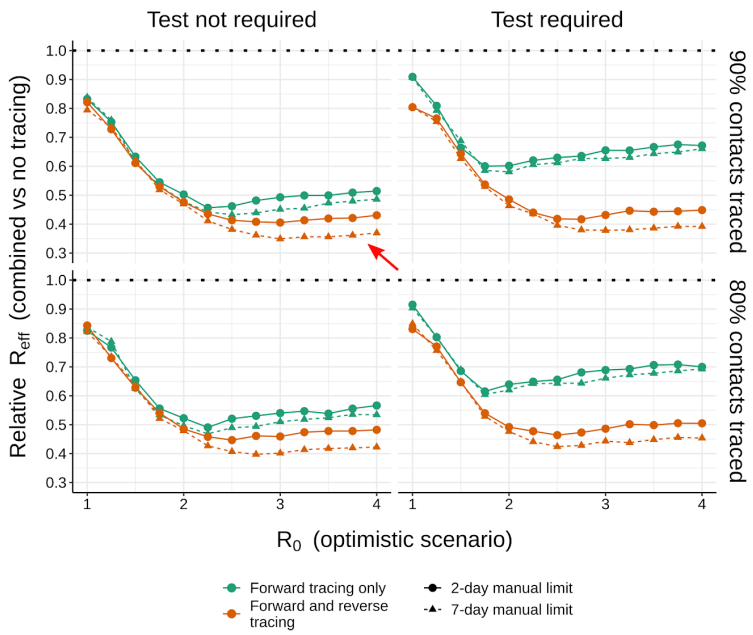

b

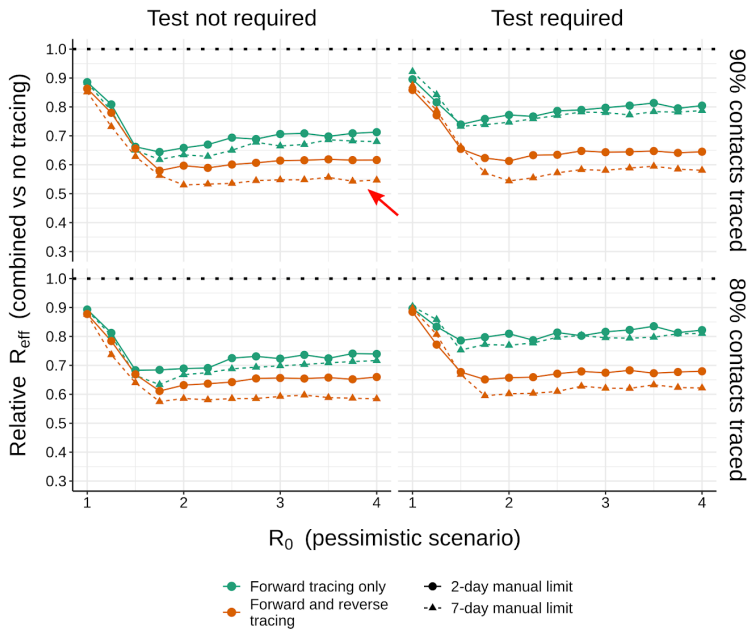

Figure S24: Relative effective reproduction number of vs no tracing (optimistic and pessimistic scenarios). Ratio between the effective reproduction number achieved by combined tracing and that achieved without contact tracing (i.e. solely under isolation of symptomatic cases) under (a) optimistic and (b) pessimistic disease parameters (Table 1), in the presence or absence of bidirectional tracing and for different rates of non-environmental contacts traced, manual tracing windows, and pre-trace testing policies for symptomatic cases. The red arrows indicate the curves corresponding to Figures 5b and 5d.

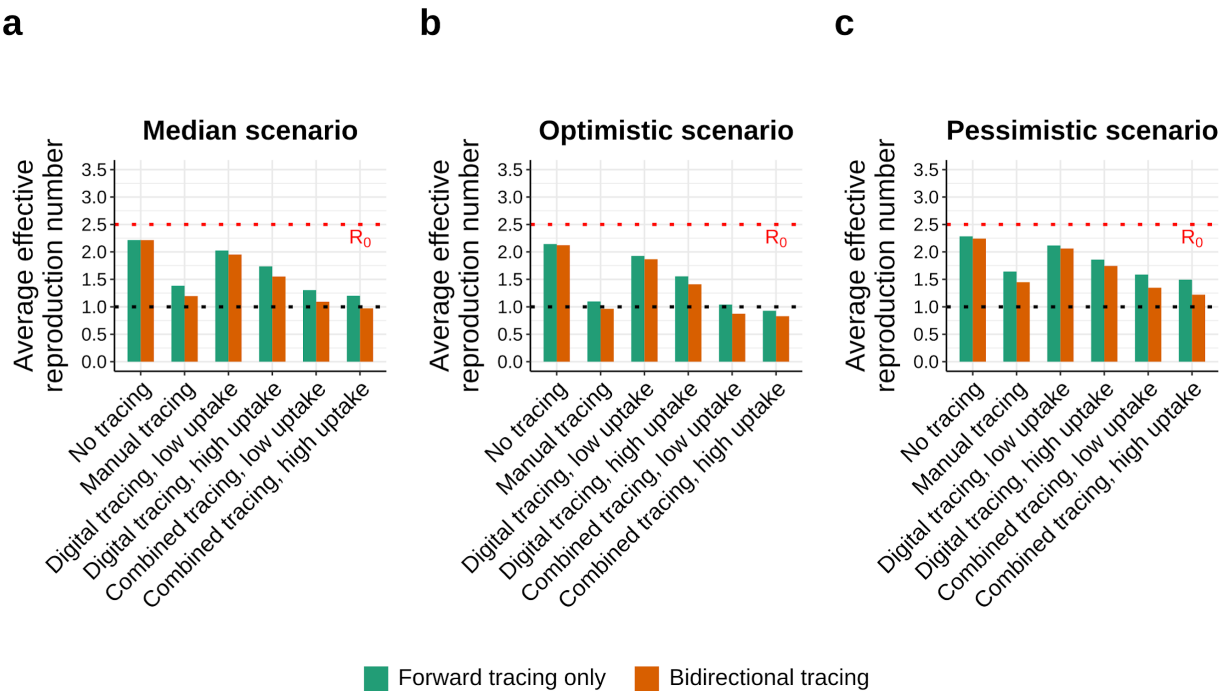

Figure S25. Tracing strategies for controlling COVID-19 (effective reproduction numbers). Average effective reproduction numbers achieved under (a) median, (b) optimistic, and (c) pessimistic scenarios (Table 1), assuming an R_0 of 2.5, 90% of non-environmental contacts traced, 7-day manual tracing windows, and immediate (pre-test) tracing of symptomatic cases. Without tracing, forward and bidirectional are equivalent.

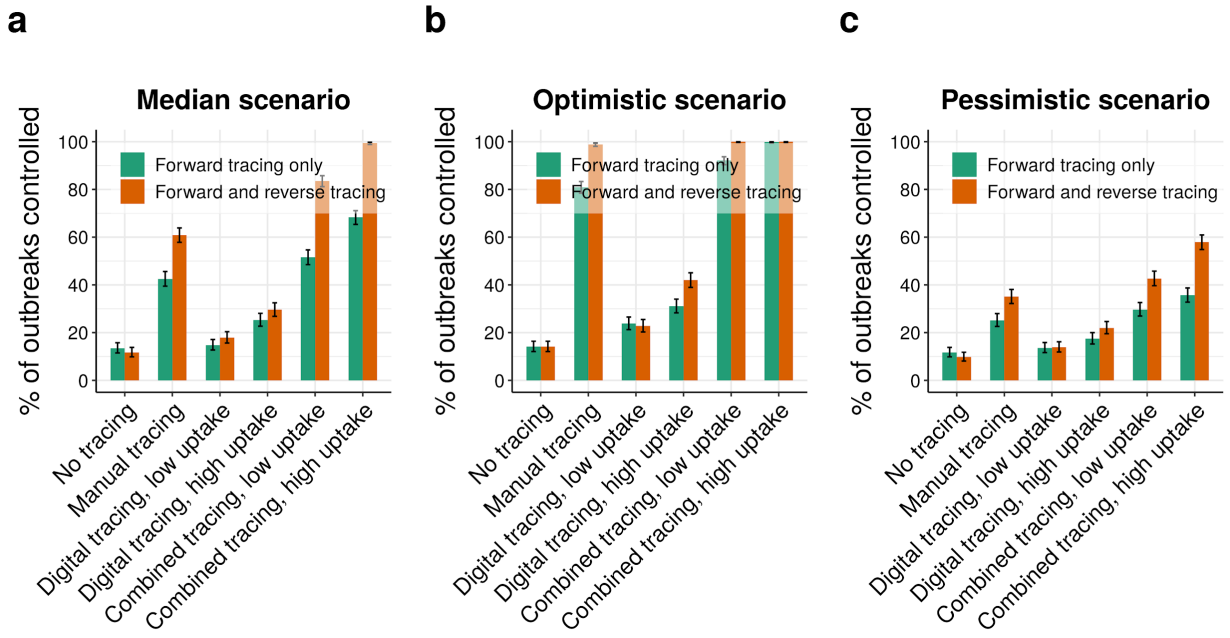

Figure S26. Tracing strategies for controlling COVID-19 (R_0 = 2.0). Rates of control achieved under median (a), optimistic (b), and pessimistic (c) scenarios (Table 1), assuming an R_0 of 2.0, 90% of non-environmental contacts traced, 7-day manual tracing windows, and immediate (pre-test) tracing of symptomatic cases. Without tracing, forward and bidirectional are equivalent.

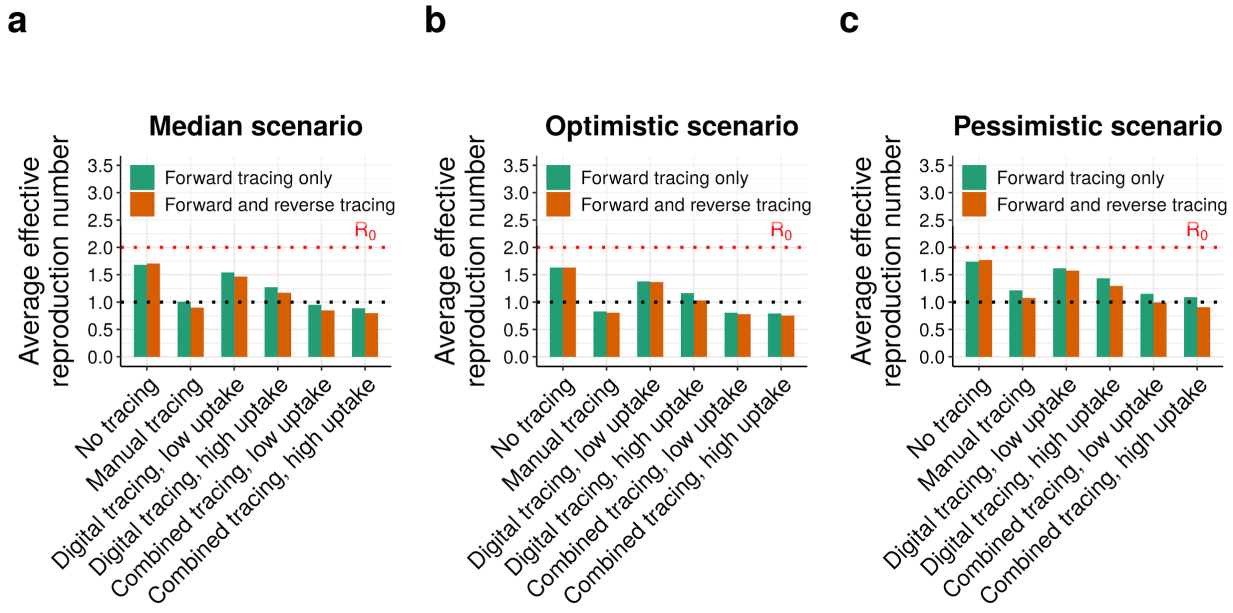

Figure S27. Tracing strategies for controlling COVID-19 (effective reproduction numbers, R_0=2.0). Average effective reproduction numbers achieved under (a) median, (b) optimistic, and (c) pessimistic scenarios (Table 1), assuming an R_0 of 2.0, 90% of non-environmental contacts traced, 7-day manual tracing windows, and immediate (pre-test) tracing of symptomatic cases. Without tracing, forward and bidirectional are equivalent.